

University of Montana

## ScholarWorks at University of Montana

---

Graduate Student Theses, Dissertations, &  
Professional Papers

Graduate School

---

1966

### Radiometric surface temperatures in relation to remote sensing of hydrologic data

Darold E. Ward  
*The University of Montana*

Follow this and additional works at: <https://scholarworks.umt.edu/etd>

**Let us know how access to this document benefits you.**

---

#### Recommended Citation

Ward, Darold E., "Radiometric surface temperatures in relation to remote sensing of hydrologic data" (1966). *Graduate Student Theses, Dissertations, & Professional Papers*. 3350.  
<https://scholarworks.umt.edu/etd/3350>

This Thesis is brought to you for free and open access by the Graduate School at ScholarWorks at University of Montana. It has been accepted for inclusion in Graduate Student Theses, Dissertations, & Professional Papers by an authorized administrator of ScholarWorks at University of Montana. For more information, please contact [scholarworks@mso.umt.edu](mailto:scholarworks@mso.umt.edu).

RADIOMETRIC SURFACE TEMPERATURES IN RELATION TO  
REMOTE SENSING OF HYDROLOGIC DATA

By

DAROLD E. WARD

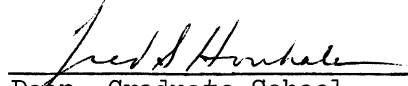
B.S.F. University of Montana, 1965

Presented in partial fulfillment of the requirements for the degree of  
Master of Science in Forestry

UNIVERSITY OF MONTANA

1966

  
Chairman, Board of Examiners

  
Dean, Graduate School

MAY 20 1966  
Date

UMI Number: EP35261

All rights reserved

**INFORMATION TO ALL USERS**

The quality of this reproduction is dependent upon the quality of the copy submitted.

In the unlikely event that the author did not send a complete manuscript and there are missing pages, these will be noted. Also, if material had to be removed, a note will indicate the deletion.



UMI EP35261

Published by ProQuest LLC (2012). Copyright in the Dissertation held by the Author.

Microform Edition © ProQuest LLC.

All rights reserved. This work is protected against unauthorized copying under Title 17, United States Code



ProQuest LLC.  
789 East Eisenhower Parkway  
P.O. Box 1346  
Ann Arbor, MI 48106 - 1346

## ACKNOWLEDGEMENTS

Sincere appreciation is extended to Professor Fred Gerlach, Committee Chairman, for his time and contribution during the planning, data collection, and the final compilation of this thesis. Without his guidance it would have been difficult to have completed this study. Dr. Robert Weidman and Professor Robert Steele, the other members of my thesis committee, were very helpful in their reviews.

The technical and professional assistance given by specific faculty members contributed substantially to this final production. Professor Melvin Morris and Dr. T. J. Nimlos made special trips to the research area on the Lubrecht Experimental Forest for the purpose of describing the vegetation and soil profiles respectively. Professor John Peterson helped in solving some of the perplexing problems encountered in writing the computer programs. Dr. William Pierce reviewed the statistics involved in the data analysis chapter.

Personnel of the U.S. Forest Service from the Northern Forest Fire Laboratory devoted considerable time in reviewing the proposed research study plan and offered constructive criticism toward improving the proposed study.

Financial assistance was provided by the Water Resources Research Office of the Department of Interior and the Forest and Conservation Experiment Station of the University of Montana Forestry School.

I owe my wife thanks for her patience, encouragement, and assistance throughout this study. Much of her time was spent in transcribing data, typing, and listening.

## ABSTRACT

Specific wavelength bandwidths within the electromagnetic spectrum are more suitable for recording special types of resource information. Remote sensors sensitive in these spectral regions are used to record the information. Electronic infrared line scanners have been developed since World War II which are capable of producing high resolution "thermal" imagery in the middle and far infrared portions of the EM spectrum. Terrain features have normal peak emission intensities in the spectral thermal emission band from 8 to 14 micron wavelengths. The land managers and research scientists thus have a tool for recording on the IR imagery heat relationships of terrain and vegetation features from remote positions. Because the tone contrasts on the IR imagery are a result of differences in infrared emission intensities between a target and its background, it is necessary for the earth scientist to understand the main physical parameters associated with a given feature producing the emission patterns. This thesis discusses the time and conditions for which the greatest differences in surface radiation-temperature exist between a gradation of moisture sites. The discussion is based on field radiation-temperature measurements.

Seven graded moisture sites were selected in a natural meadow environment within the Lubrecht Experimental Forest which is managed by the University of Montana School of Forestry. The vegetational composition, soil profiles, and the general geology for the area are described. Surface radiation-temperatures were collected for the

seven sites on a diurnal basis for five days during the month of October, 1965 using a Stoll-Hardy HL<sup>4</sup> Radiometer. A systematized sampling procedure was employed for each site thus repeating the temperature measurements for specific sample points.

By applying standard statistical methods the differences in surface radiation-temperature means between sites were evaluated. It was found that the greatest differences in surface temperature as correlated to soil moisture occurred during peak insolation receipt periods. Certain meteorological conditions were found to be important considerations in determining the best imagery collection periods. Both single and double factor regression analysis procedures were applied to the data for the purpose of determining the effect of microslope and aspect as well as variable grass height on surface radiation-temperature variation within a given moisture site. The effect of microslope and aspect differences are a major source of variation within the radiation-temperature samples for a given site and time. The effect of slope and aspect is analyzed using angles of insolation incidence. Also, the slopes of the regression lines for this variable are seen to be correlated to meteorological conditions. This is a preliminary investigation into some of the problems involved in interpreting moisture related features from IR imagery.

TABLE OF CONTENTS

	PAGE
I. INTRODUCTION .....	1
OBJECTIVES .....	4
II. LIBRARY RESEARCH .....	5
FACTS ABOUT INFRARED .....	5
LITERATURE REVIEW .....	7
III. RESEARCH PROCEDURES AND SITE DESCRIPTIONS .....	12
SELECTION OF A STUDY AREA .....	12
SITE SELECTION AND SAMPLING THEORY .....	14
VEGETATIONAL COMPOSITION BY SITE .....	17
SOILS AND GEOLOGY .....	21
SOIL MOISTURE .....	25
RADIATION-TEMPERATURE MEASUREMENTS.....	27
IV. DATA ANALYSIS AND DISCUSSION .....	32
RADIATION-TEMPERATURE GRAPHS .....	33
DETERMINATION OF THE BEST IMAGERY COLLECTING TIME .....	35
VARIATION WITHIN SITES RESULTING FROM GRASS HEIGHT .....	40
VARIATION WITHIN SITES RESULTING FROM MICROSLOPE AND ASPECT DIFFERENCES .....	44
INFERENCE OF THE EFFECT OF MAJOR SLOPE DIFFERENCES ON RADIATION-TEMPERATURE .....	48
MULTIPLE REGRESSION ANALYSIS .....	50
ANALYSIS OF SAMPLE POINT DEVIATES .....	54
V. CONCLUSIONS .....	58
VI. BIBLIOGRAPHY .....	60

TABLE OF CONTENTS (Continued)

	PAGE
VII. APPENDIX:	
A. FILTER SPECTRAL ANALYSIS .....	64
B. WEATHER SUMMARY .....	66
C. DETERMINATION OF ANGLE OF INSOLATION RECEIPT FOR INDIVIDUAL SAMPLE POINTS .....	71
D. PHOTOGRAPHS OF FEATURES .....	77
E. GRAPHS OF MEAN R-T VALUES .....	83
F. ADJUSTMENT OF R-T MEANS .....	89
G. GRAPHS OF THE PEAK INSOLATION RECEIPT PERIODS .....	90
H. GRAPHS OF REGRESSION EQUATIONS .....	96
I. SCATTER DIAGRAMS OF R-T DEVIATES .....	102



LIST OF TABLES

TABLE		PAGE
1	Grass species present as indicators of soil moisture..	17
2	Average grass height in inches for each sample point on each of the seven sites .....	18
3	Vegetational composition of each site .....	19
4	Soil profile abbreviated descriptions .....	24
5	Percent moisture content for each site measured at the two-inch level .....	26
6	Master table for the analysis of variance and a de- scription of Duncan's multiple range test .....	36
7	Significance of differences between site means for 13 different time periods. Also, listing of parameters used in defining the best IR imagery collection period .....	38
8	Equations for regression lines. Wind and cloud cover are also listed .....	46
9	Minimum difference in surface R-T which may occur between north and south slopes for each of the five sample days .....	49
10	Listing of multiple regression analysis equations ....	51
11	Weather data from the Greenough Post Office Weather Station for October, 1965 .....	67
12	Weather data collected at the Lindbergh Meadow Weather Station for October, 1965 .....	68
13-14	Hourly weather data for each of the five sample days .....	69
15	Angle of insolation incidence for each sample point by time .....	75

## LIST OF FIGURES

FIGURE		PAGE
1	Telephoto view of the Lindbergh Meadow, study location...	14
2	Diagram of systematized sampling format used on each site .....	16
3	Geologic map of Lindbergh Meadow and vicinity .....	21
4	Photograph of the soil profile for site I .....	23
5	Photograph of the soil profile for site II .....	23
6	Photograph of the soil profile for site V.....	23
7	Stoll-Hardy HL4 Radiometer used for collecting surface R-T data features .....	28
8	Demonstration of method for using Stoll-Hardy radio-meter in collecting data .....	28
9	Form for recording field R-T data .....	9
10	Graph showing difference in R-T between the natural grass sites and the corresponding paired clipped sites.....	42
11	Photograph of sample point 1 on site VII showing grass density .....	43
12	Photograph of sample point 11 on site VII showing grass density .....	43
13	Regression lines for five days (R-T as a function of angle of insolation incidence for site I from 1300 to 1400) .....	47
14	Regression lines for five days (R-T as a function of angle of insolation incidence for site IV from 1300 to 1400) .....	47
15	Photograph of sample point 3 on site IV showing the high albedo .....	56
16	Photograph of sample point 6 on site IV showing a lower albedo than point 3 .....	56
17	Spectral response curve for the infrared filter used on the Stoll-Hardy radiometer .....	65

LIST OF FIGURES (Continued)

FIGURE		PAGE
18	Sample plot geometry .....	71
19	Bearing and elevation of sun as a function of time...	74
20	Deviation in angle of insolation incidence from a horizontal plane as a function of angle from the direction of aspect and the sun's inclination .....	74
21-27	Photographs of sites I through VII .....	78-80
28	Photograph of the reservoir's edge .....	80
29	Photograph of quartzite boulder .....	80
30	Photograph of stream which discharges into reservoir.	81
31-35	Photographs of clipped paired plots .....	81
36-40	R-T as a function of time by sites for the five data collecting days .....	84
41	Adjustment of R-T means to one point in time .....	89
42-46	Expanded scales for R-T as a function of time for the five data collecting days for the peak insolation receipt periods .....	91
47-51	Regression lines for R-T as a function of angle of insolation incidence for site IV for all five data collecting days .....	97
52-56	Deviation in R-T from the sample mean for each sample point on site IV by time for all five data collecting days .....	103

## I. INTRODUCTION

A need for new techniques for gathering information about water resources arises through the demands for greater volume, continuous supply, and improved quality of water. In the past two decades developments in the electronic and photographic fields have presented approaches to more rapid acquisition of many kinds of resource information. There are efforts being made toward further expansion of these capabilities by attempting to equate water resource information on the ground to data accumulated from remote positions. Considerable progress has been made in the past toward providing the researcher and the land manager with valuable tools for reducing the labor and time involved in acquiring water resource data. For example, by using normal panchromatic air photography it is possible to assemble data such as the area of watersheds, geologic structure maps, soil type classifications, stream gradients, water depths, stream cross sectional areas, drainage patterns, water pollution, the selection of catchment basins, instrumentation sites, and a host of other data.

The above accomplishments are only a beginning. In more recent years, new techniques for obtaining information utilizing electromagnetic radiation from outside the visible portion of the spectrum have been developed which have the potential for implementing extended resource understanding. Radar sensing devices with their all weather imaging capability have extended the field of remote sensing into the centimeter wavelength regions. These microwave sensors have the penetration potential necessary for revealing subsurface phenomena such as

ground water tables, moisture content of soils, compaction of soils, and soil texture. Other remote sensors are being used in the shorter than visible wavelengths. Gamma ray sensors can detect thorium, uranium and potassium deposits. X-rays are used for seed evaluation and for detecting insects in agricultural grains. Infrared imaging devices have capabilities of detecting and recording on film small changes in temperature. Some have reported distinguishing differences of  $0.01^{\circ}\text{C}$ . depending on the sensitivity of the scanner system employed. Within the visible spectrum new multispectral capabilities have been developed for recording up to nine different images simultaneously photographed using different portions of the visible and near infrared spectrum for activating the sensory films. Combinations of any of the above might be employed simultaneously. The state-of-the-art developments in sensing equipment is far ahead of the researcher's ability to understand what is being imaged.

Remote sensing by infrared line scanning techniques is only in its infancy. Little is known regarding possible applications of this sensing device. Many organizations, especially military financed research organizations, have collected imagery of different natural and cultural features. However, no major attempt has been conducted to determine the practicability of interpreting one set of features from IR (infrared) imagery versus some other remote sensing medium. Little is known about the time when the greatest temperature differences might be expected between selected targets and their backgrounds.

Sensing in the near and middle IR spectral range (.76u to 15u) could prove extremely advantageous in exploring temperature environments

for the purpose of energy exchange relationships or for deducing other phenomena correlated with temperature. Past interpretation work with IR imagery has demonstrated that some moisture related features can be deduced by their emission characteristics. Photographic infrared has also been noted for its moisture sensing quality. As with all interpretation work, the tone representation of an image is a result of the many physical relationships involved in the object's environment. The major contributing factors must be recognized in correctly identifying a detectable image recorded from a complex environmental situation.

In wild land studies, many variables are presented which tend to shadow or obscure particular emission patterns for specific details. An example of this follows. A warm water spring on a south exposure will appear differently on IR imagery than it would on a north slope. Even though the spring is at a constant temperature on both slopes, the background will vary between slopes and it may be impossible to distinguish the spring from its background in one case because of this. However, it can probably be deduced, if the springs can be identified, that these two springs have nearly equal temperatures by understanding the factors contributing to the background temperatures and adjusting the interpretation judgement accordingly. Under certain conditions a spring could appear light toned on a north slope and dark toned on a south slope in relation to its background temperature. Maybe the importance of the interpretation is that the two springs were correctly identified as springs in both cases.

There are many other possible types of information about water resources which may be realized from IR imagery. Evaporation and

transpiration relationships are directly related in the energy system to absorption and transfer of heat away from and into the soil. This has a special ramification in changing the surface temperature which in turn changes the amount of re-radiation from a surface in order that an energy equilibrium might be maintained.

#### OBJECTIVES

The objectives of this study are based on a need for learning more about interpreting water related features from IR imagery. There has been little work directed toward specifically identifying and measuring radiation-temperatures \* of selected ground features. The objectives of this study can be stated as follows:

- (1) To observe and describe the relative R-T differences for selected moisture sites.
- (2) To infer the conditions and time for which the greatest R-T differences exist between the selected moisture sites.
- (3) To define some of the variables present within each moisture site which may tend to obscure the identity of the site on IR imagery.

---

\*Radiation-temperature will be abbreviated as R-T throughout the remainder of this paper. Surface temperatures recorded by the Stoll-Hardy Radiometer are a function of the amount of radiation emitted by an object in the spectral range from 3 to about 25 microns.

## II. LIBRARY RESEARCH

### FACTS ABOUT INFRARED

The electronic infrared recorder referred to previously as capable of producing IR imagery is correctly termed an Electronic Infrared Line Scanner. This airborne infrared scanner consists of a rotating mirror which collects radiation from the earth's surface along a narrow path normal to the flight direction. This radiation is reflected to the surface of a parabolic mirror which concentrates the collected energy while reflecting it onto a solid state detector. The output of the detector is amplified and this signal modulates the output of a cathode ray tube which directs a beam of electrons across a film at right angles to its direction of movement. The radiation received by the detector determines the intensity of the beam of electrons. There exists a correspondence between the intensity of radiation from objects on the ground and the final tone representation on the film. The forward movement of the plane corresponds to the rate at which the film is pulled across the cathode ray tube opening, thus recording a line by line strip image of the ground radiation.

Since the terrain is not photographed directly by the infrared sensor, the term "infrared imagery" is used to describe the final photograph obtained. A remote sensor is an instrument or device used for the measurement of some property of an object without physical contact between the measuring device and the object. In the case of quantifying infrared energy relationships of terrain detail by an airborne remote sensing device, one encounters many variables which affect the intensity



of the infrared radiation reaching the recorder. All variations in the amount of radiation emitted by various components of the terrain are traceable to differences in either emissivity or temperature or combinations of both (First Symposium, 1962). Temperature variations may be a function of one or more of the following:

- (1) wind, (2) heat capacity, (3) thermal conductivity,
- (4) surface to volume ratios, (5) moisture content and the evaporation processes, (6) sky cover and its effect on radiation exchange, (7) topography and solar history,
- (8) elevation differences and the thermocline, (9) Metabolism of plants, and (10) dewfall and precipitation.

Colwell (1963) describes many of the physical parameters involved in remote reconnaissance work. Emissivity coefficients for terrain detail range from .70 to 1.00 where emissivity is a constant for a given object for a given wavelength and represents the rate of emission of radiation for that object. The object's molecular and atomic structure determines the wavelength and rate of emission of electromagnetic energy. The electromagnetic energy is reflected, scattered, absorbed and emitted by an object according to its physical properties. A blackbody absorbs all incident radiation and subsequently re-emits the same amount of radiation. Terrain details can be considered as gray bodies which have varying emissivity percents. All radiation reaching the detector from these varying intensity emitters is a function of the inverse square of the path distance. The radiation law describing the intensity of emission from an object is given by

$$R = \epsilon \sigma T^4 \text{ where}$$

- R = the total energy radiated in watts per meter<sup>2</sup>,
- $\epsilon$  = the emissivity coefficient,
- T = the absolute temperature of the object in degrees Kelvin,
- $\sigma$  = the Stefan-Boltzmann constant ( $5.67 \times 10^{-8}$ ).

Cantrell (1964) claims that reflected solar energy is less desirable than emitted energy for differentiating the physical character of terrain features. Solar reflections peak at a wavelength of 2 microns whereas the earth has a radiant power peak near 9.6 microns and a mean temperature of 300 degrees Kelvin. For these reasons, it is desirable to use a heat mapping device sensitive to radiation in the 8 to 14 micron range. Cantrell and others have reasoned that emitted energy is more characteristic of soil moisture, and geologic features than reflected radiation.

#### LITERATURE REVIEW

There is little literature available regarding the application of infrared imagery to the collection of hydrologic data. It has been suggested by Pryor (March, 1964) that infrared imagery supplemented by normal photography may have potential benefits for increasing the reliability of the photo interpreter's judgements. Several groups have demonstrated the usefulness of infrared imagery as a data collecting media for geological information. Fischer and associates (1964) utilized an infrared scanner for delineating volcanic zones on the Hawaiian Islands. They measured the air temperature and the surface temperature of several objects with a contact pyrometer and recorded these data in graphical form. The temperature changes from 0200 to 1000 hours were measured since this was the period during which they expected the greatest contrast to occur between the volcanic fringes and their natural surroundings. Ground truth information has been collected for selected sources during IR thermal imagery collecting missions at the University of Michigan in their Multispectral Data Collection Program (Lowe, 1964).

The measurements were made using thermocouples; however, plans for the future at that time included using a radiation thermometer sensitive in the 8 to 14 micron spectral range.

Cantrell (1964) summarizes the application of IR imagery to various geologic interpretation problems. He stresses the importance of determining the proper conditions for collecting the imagery depending on the specific purpose for which it is to be used. The earth is at its highest relative terrain emission immediately after sundown which appears to be the best time for collecting IR imagery of rock formations. However, there are other features especially those under vegetative cover which may maintain a longer period of maximum radiation emission. It has been theorized by Cantrell that certain geologic features may superimpose their radiation patterns on the overhead vegetation by building up "heat sinks" directly under the canopy. (From an examination of IR scanner imagery, it is seen that some hydrological features may produce "hot or cold sinks.") Thus the vegetation may reradiate the characteristic radiation from the feature. If this reasoning is sound, then still nights when the wind is not disrupting the heat sink formation would seem to be the best time for collecting IR imagery of terrain features covered by vegetation. Cantrell illustrates examples where IR imagery has been used to delineate marshy areas and drainage patterns of streams. He doesn't elaborate on the efficiency of IR imagery compared to air photography as a media for interpreting these features.

Leonardo (1964), Harris (1964), Udall (1965), and Cantrell (1964) all stress the important advantages of using IR recording devices

for collecting temperature differential data from large bodies of water. Udall tells how cool water springs were identified in coastal waters near Hilo, Hawaii using IR imagery. Oshiver and Berberian (1965) compared ship and airborne R-T observations in an effort to establish atmospheric attenuation data and calibration data for airborne infrared detectors used for isothermal mapping studies of sea surfaces.

IR imagery was utilized by Lattman (1963) for delineating warm water springs along valley margins. He claims that cool air may flow down valley bottoms early in the evening causing a rapid transmission of the radiation from the valley floor which later in the evening will appear dark toned on the IR imagery. He states that the differences between sandstone and shale recorded on the imagery are caused by different specific heats for the two physical substances. This resulted in uneven heating during the preceding day, and therefore different temperatures existed for the separate features at night when the imagery was produced. Some of the recorded temperature variations between the two rock features were attributed to differences in vegetative cover. No description of the vegetation or temperature regimes was given by Lattman.

A good example of differences in emissivity and its effect on radiation emission was demonstrated by Harris (1964) for a plowed field contrasted to an unplowed field. He failed to mention in the text whether plowed fields are higher emitters of radiation or if the unplowed region appears the lightest toned on the resultant imagery. The relative contrast in this comparison may depend on the time when

the imagery was obtained.

Ory (1964) suggests that dark toned images of stream drainage patterns indicate a high concentration of surface and sub-surface moisture. He indicates that these images are a result of the moisture concentrations and resultant vegetation. Other examples of IR imagery are presented showing clear delineation of swales and contrasting moisture sites. No mention is made regarding the collection time or meteorological conditions for IR imagery.

A graph from a Syracuse University Research Institute report reproduced by Suits (1960) demonstrates the different radiation intensities in relation to wavelength for grass, concrete, red brick, and snow. All substances were at approximately the same ambient temperature, 4 degrees centigrade. Suits states that it is the differences in area under the curve for each substance that must be differentiated before a recognizable image can be produced. Suits claims that the atmosphere tends to alter the inherent radiation emitted from objects on the ground since it too emits and absorbs infrared energy. Colwell (1963) theoretically confirms this result. Gates (1964) shows graphs indicating significant differences in the temperature relations between warm water springs, moss, bare soil, snow, air, and sky during the winter in Yellowstone Park.

Gates (1964) has developed equations defining the factors contributing to leaf temperatures for broadleaf and conifer species. From these considerations, he has deduced that conifers should appear cooler or darker toned on IR imagery during periods of high solar insolation receipt than the broadleaf species. This condition is reversed on

nighttime thermal imagery. Gates feels that "...careful consideration of the basic properties of the surface, including the characteristics of soils and plants, will lead to a systematic interpretation of aerial reconnaissance records." Colwell and Olson (1964) suggest that careful consideration be given to the time of day, type of terrain, and weather conditions in defining the thermal imagery collecting period and in interpreting the IR imagery.

There may be other classified sources of information relating to more specific aspects of interpretation of terrain features from IR imagery. This literature review summarizes the significant work to date. A general comment about the work in this field is that little effort has been indicated in regard to obtaining ground truth about terrain features.

### III. RESEARCH PROCEDURES AND SITE DESCRIPTIONS

#### SELECTION OF A STUDY AREA

IR imagery interpretation involves deductions as to the surface temperatures expected for a given feature and its background in a known environmental situation. Necessarily the interpreter must have considerable biological and physical scientific background to comprehend the complex environmental situations possible. Many interpretation problems can be solved from past interpretation experience. This is one approach in learning to interpret features from IR imagery. In other words, one might collect considerable IR imagery of one set of features under various time and environmental conditions, then deduce image characteristics. This study is oriented toward the other approach which involves actual ground verification of R-T signatures in relation to identifiable environmental conditions. The ground truth information obtained can then be compiled and used for reference in making interpretation judgements from IR imagery.

Since this study relies entirely on ground control data, the logical approach was to select an area with as much information already assembled as possible. However, it is considered desirable to maintain this study under natural field conditions. The following criteria were considered in selecting the study location:

- (1) It would be desirable to have geologic map coverage for the selected area.
- (2) It would be desirable to have continuous weather data and past weather history data available.
- (3) The selected area should contain examples of the following features:

- (a) Rock outcrops.
  - (b) Swale and swampy sites.
  - (c) Springs and surface seepage areas.
  - (d) Both wet and dry meadows.
  - (e) Streams of different sizes under various cover conditions.
- (4) The features found on the selected area should be typical of other areas.
- (5) The study location should be accessible both by vehicle and on foot.

By examining current panchromatic air photography of the entire Lubrecht Experimental Forest, the possible study locations were selected on the basis of how well they conformed to the above standards. Then an extensive ground survey of these likely sites was conducted and an area chosen which contained typical site features with considerable variation between features.

The area selected is located on a privately owned meadow surrounded by University of Montana Forestry School property, section 12, T.13 N., R.15 W. (Figures 1 and 3). Permission was obtained from Mr. Land Lindbergh to establish site plots on his property. This meadow area contains extremes in moisture sites plus the advantage of having these various sites located within a fifteen minute walk of one another. Some of the features located on the selected area are both mesic and hydric type conditions, a small stream, a two-acre reservoir, a large quartzite boulder and various surface seepage conditions. The features are located under near uniform insolation conditions. Present ecological disturbances are limited to grazing by cattle. The microclimatic conditions, vegetational composition and the type of features present are similar to that on other mountain valley meadow



lands. Continuous weather data is recorded at the Greenough Post Office located about one mile from the study site.

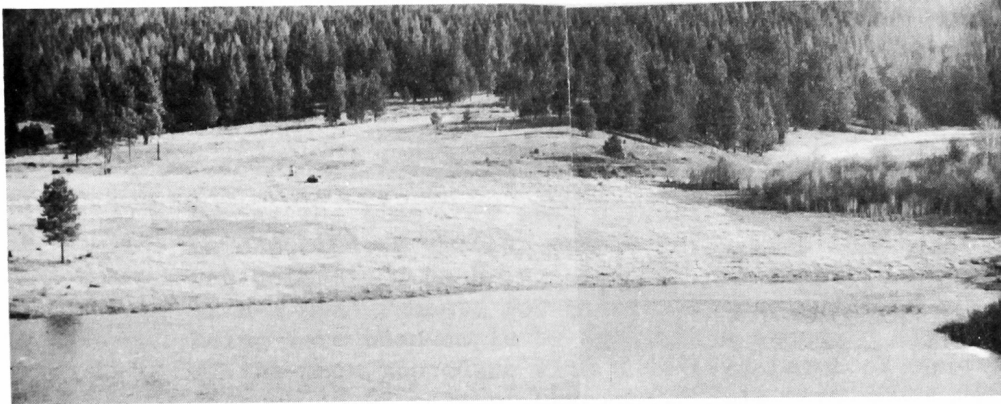


Figure 1. Telephoto view of the Lindbergh Meadow study location.

#### SITE SELECTION AND SAMPLING THEORY

Evapotranspiration and energy exchange studies indicate a high correlation between soil moisture and surface soil temperature. However, little information is available regarding surface R-T and moisture relationships under natural meadow conditions. Therefore, it was necessary to explore these anticipated differences; this was done with a Stoll-Hardy Radiometer (See description on page 27). The initial sampling was accomplished by establishing five transect lines over five different moisture sites. Along each of the five lines, twenty random selected points were sampled with the radiometer.

The original R-T data for the five sites indicated that there is a strong relationship between soil moisture and R-T under meadow conditions. In fact, an F ratio of 188 was obtained by analysis of variance for the differences in R-T means between sites. Thus, the differences between means are significant at the 99 percent level of confidence. Several changes were adopted based on these original data:

- (1) During the time when peak differences in R-T might be expected, a smaller sample size (less than 20) was determined as being adequate. A sample size of 12 R-T measurements for each site was indicated as being more than ample by applying a standard error of the mean procedure with a desired level of confidence of 95 percent that the sample mean would not vary by over 5 percent from the true population mean (Pierce, undated).
- (2) It was decided to increase the number of moisture sites from five to seven. These sites were selected on the basis of soil moisture in the top six inches of soil. Consideration was given in locating the sites to select typical ecological units (Figures 21 to 27).
- (3) In addition to the seven major sites, three secondary sites were sampled including a large quartzite boulder, a small stream, and the edge of a two-acre reservoir (Figures 28 to 30).
- (4) A systematized sampling procedure was adopted replacing the line sampling method. It is easier to statistically separate more variables if identical plot points are sampled during each sampling period. The sample points were arranged in a pattern shown by Figure 2 and oriented in a north-south direction. Orientation in a cardinal direction was considered necessary to permit the researcher to sample each site similarly. Thus, the possibility of shading the plot point before sampling the R-T was reduced.
- (5) It was determined advisable to always walk between the two rows of stakes and sample with the radiometer toward the outside where the circles are diagrammed on Figure 2. This was done to avoid disrupting the natural vegetation and environment of the sample points.

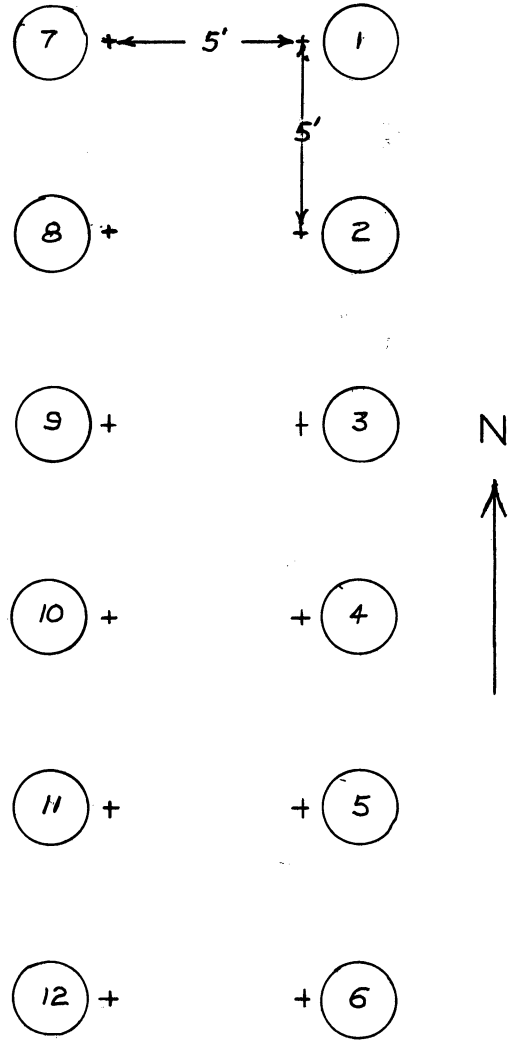


Figure 2. Diagram of sampling formation used on each site.

VEGETATIONAL COMPOSITION OF SITES

The vegetation growing on a site is a result of the available moisture, nutrient composition, soil condition, and the solar energy available. Under wildland conditions, one usually finds similar vegetation growing on near uniform sites. The amount of vegetative material present on a site is an indication of the site quality. Both vegetational composition and the amount of plant material present on a site affect the evapotranspiration rates as well as the amount of absorption of incident solar radiation.

It is considered that even though the plant composition is variable between selected sites (Table 3), the species present are representative of the moisture regimes by site. This was verified by Professor Melvin Morris from the University of Montana School of Forestry who compared the grass species present on each site to a list of indicator species of soil moisture. This list (Table 1) was compiled from his personal experience in soil moisture-vegetation analysis work for other areas of Montana.

TABLE 1. GRASS SPECIES INDICATING SITE MOISTURE CONDITION

Site description	Indicator vegetation present
(1) Very wet site (slow water movement on surface)	Pure sedge.
(2) Wet (water movement evident, spongy, water at surface early in growing season)	Sedge, Tufted hairgrass, Redtop.
(3) Moderately wet (water table near surface)	Redtop, Sedge, <u>Juncus</u> sp.

TABLE 1. (continued)

Site description	Indicator vegetation present
(4) Good moist site.	Timothy, Bluegrass, Potentilla, Dutch clover.
(5) Driest site.	Bluegrass, Pussytoes, Yarrow.

Other vegetative parameters varied between sites and within each site. Table 2 shows the grass height variation for each of the R-T sample points. These grass height values represent the average

TABLE 2. AVERAGE GRASS HEIGHT IN INCHES FOR EACH SAMPLE POINT

Site	Sample points											
	1	2	3	4	5	6	7	8	9	10	11	12
I	0.5	4.0	1.0	1.0	1.0	1.5	1.0	2.5	1.5	1.0	1.5	1.0
II	1.0	1.5	1.0	1.0	1.0	1.0	1.0	1.0	1.0	1.0	1.0	1.0
III	2.0	8.0	8.0	8.0	6.0	8.0	8.0	8.0	6.0	4.0	6.0	3.0
IV	1.0	1.0	1.5	1.0	1.0	1.0	1.0	1.0	1.5	1.5	1.0	1.5
V	1.0	1.0	1.0	1.0	1.0	1.0	1.0	1.0	1.0	1.0	1.0	1.0
VI	1.0	2.0	1.0	1.0	6.0	1.5	1.0	6.0	1.0	8.0	1.5	1.5
VII	6.0	2.0	6.0	1.0	2.0	1.0	1.5	3.0	3.0	4.0	2.0	2.0

grass height in inches for each plot point. The intensity of grazing by range cattle is one of the factors which has altered the vegetation height and the ecological development. However, the meadow has not been grazed excessively and this is not considered by this author to have created an unnatural condition. It is felt that it is one of the factors affecting surface R-T which must be understood rather than avoided by fencing the plots. The surface albedo varied between sites and was one of the uncontrolled parameters in this study. It is known

that the albedo is higher for sites I and IV than for site II. The vegetation density was lower for sites I and IV than for the other sites. This is primarily a result of low soil moisture on these two sites. Geiger (1957) indicates that bare loose soil and soil covered by loose organic material reaches a higher surface temperature than green vegetation. Hence, the absence of 100 percent cover on sites I and IV only tends to increase their dominant temperature position.

TABLE 3. SPECIES COMPOSITION BY SITE\*

<u>Site I</u>		
80%	Poa pratensis	Kentucky bluegrass
15%	Potentilla Sp.	Five-fingers
		Glandulosa
5%	{ Bromus Sp.	
	{ Rumex Sp.	
	{ Achillea Sp.	Yarrow
<u>Site II</u>		
35%	Agrostis Sp.	Redtop
10%	Poa pratensis	Kentucky bluegrass
15%	Trifolium repens	Dutch white clover
5%	Juncus balticus	Rush
15%	Phleum pratense	Timothy
20%	{ Carex nebraskensis	Sedge
	{ Taraxacum officinale	Common dandelion
	{ Potentilla Sp.	Five-fingers
	{ Achillea Sp.	Yarrow
<u>Site III</u>		
50%	Agrostis Sp.	Redtop
1%	Juncus balticus	Rush (Without bracts)
3%	Juncus longistylus	Rush (With bracts)
5%	Phleum pratense	Timothy
10%	Deschampsia caespitosa	Tufted hairgrass
30%	Carex nebraskensis	Sedge
1%	{ Poa pratensis	Kentucky bluegrass
	{ Trifolium repens	Dutch white clover
<u>Site IV</u>		
90%	Poa pratensis	Kentucky bluegrass
5%	Potentilla Sp.	Five-fingers
4%	Achillea Sp.	Yarrow

TABLE 3 (continued)

		<u>Site IV (continued)</u>
1%	{ Phleum pratense Agropyron Antennaria rosea	Timothy Timber wheatgrass Moss
		<u>Site V</u>
40%	Agrostis Sp.	Redtop
15%	Poa pratensis	Kentucky bluegrass
20%	Trifolium repens	Dutch white clover
3%	Potentilla Sp.	Five fingers
5%	Phleum pratense	Timothy
10%	Junculus longistylus	Rush (With long bract)
5%	Carex nebraskensis	Sedge Moss
		<u>Site VI</u>
45%	Agrostis Sp.	Redtop
30%	Carex nebraskensis	Sedge
10%	Juncus balticus	Rush
10%	Trifolium repens	Dutch white clover
5%	{ Phleum pratense Potentilla gracilis Geum Sp.	Timothy Five-fingers
		<u>Site VII</u>
85%	Carex nebraskensis	Sedge
15%	Agrostis Sp.	Moss Redtop
	Deschampsia caespitosa	Tufted hairgrass
	Muhlenbergia Sp.	

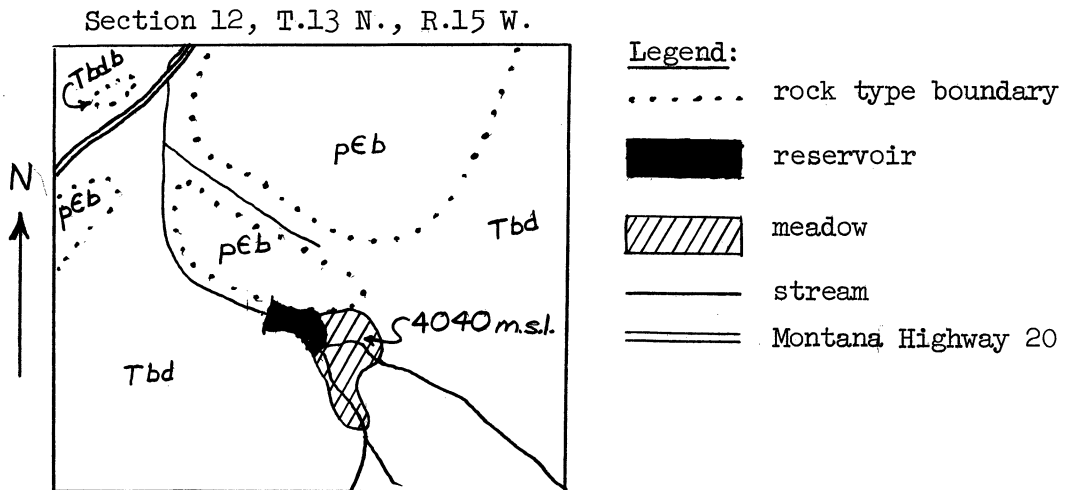
\*Percentage values were estimated after careful ocular examination of each site by Professor Melvin S. Morris, School of Forestry, University of Montana.

### SOILS AND GEOLOGY

The structure, texture, color, number and size of coarse fragments, amount of organic material, characteristic moisture condition, and other soil factors are important in determining the rate of thermal diffusivity and the heat capacity for a given soil profile. Chudnovskii (1948) and Buckman (1959) both indicate the dominant roll of soil moisture in determining the surface R-T for a soil.

The characteristic parent materials for the soils on the Lubrecht Experimental Forest are discussed by Brenner (1964). The underlying rock types as mapped by Brenner are shown in Figure 3. He describes the

Figure 3. Geologic map of the Lindbergh Meadow and vicinity



Tbd	Basin deposits (Tertiary)
Tbdb	Breccia and Felsite (Tertiary)
pEb	Bonner quartzite (Precambian)



Tertiary basin deposits as appearing to be horizontally bedded and consisting of "...poorly consolidated mudstone, sandstone, and conglomerate." Few outcrops of these materials were found by him within the School Forest. Decomposition of the fine textured materials have likely resulted in the fine textured soils found in the meadow.

It is felt that the abbreviated soil profile descriptions in Table 4 might be useful in relating this study to others. Dr. T. J. Nimlos (1966) examined the soil profiles for the three major moisture divisions and described the soil profiles for sites I, V, and VII as listed in Table 4.

Soil pits were not excavated for all sites. However, a pit was examined for site II and proved to have nearly an identical soil profile to that for site V except that the coarse fragments were larger on site II (Figures 5 and 6). Site VI was located near site V and was considered to have the same soil profile. Site IV was observed to be similar to site I by examining soil pits on the respective sites (Figure 4). Site III has near identical soil characteristics to site VII except the organic matter level is lower and not of a sedge vegetation type on site III. There is evidence of a sub-surface glei horizon for site III which is similar to that noted on site VII.



Figure 4. Soil profile photograph for site I. Site I is similar to site IV. See Table 4 for a description of horizons. This is a Lubrecht loam soil profile.



Figure 5. Soil profile photograph for site II. Site II is similar to site V. This is a humic gley soil profile.



Figure 6. Soil profile photograph for site V. See Table 4 for description of horizons. This is a humic gley soil profile.

TABLE 4. SOIL PROFILE ABBREVIATED DESCRIPTIONS\*

<u>SITE I.</u>		Soil profile is a Lubrecht loam (Figure 4). The profile shows signs of recent deposition. This is a moderately well drained site.
A1	0-5"	Very dark brown (10YR 2/2) silt loam; weak fine granular structure; much evidence of mixing, charcoal present.
B1	5-12"	Brown to dark brown (10YR 4/3) silt loam; weak coarse blocky structure; a few mottles present.
BT	12-16"	Brown to dark brown (10YR 4/3) silty clay; moderate medium blocky structure; a few fine mottles present.
BD	16-21"	Dark yellowish brown (10YR 4/4) clay; coarse and strong structure; numerous mottles present; 30 percent coarse fragments of subrounded quartzite less than 3 inches in diameter; B horizon with some development.
<u>SITE V.</u>		Soil profile is a humic glei (Figure 6). The soil is poorly drained, but not as much organic matter as on site VII.
O2	0-2"	Black (10YR 2/1) silty loam; organic horizon; abundant fine roots.
A1	2-10"	Black (10YR 2/1) silty clay; moderate medium granular structure; common fine roots.
G	10-22"	Light brownish gray (2.5Y 6/2) silty clay loam; moderate medium blocky structure; 40 percent coarse fragments of subrounded quartzite less than 4" diameter, numerous fine mottles.
<u>SITE VII.</u>		Soil profile is a humic glei. The sedge peat soil is very poorly drained with standing to moving surface water present.
O2	0-6"	Very dark grayish brown (10YR 3/2) peaty; very abundant fine and medium sedge roots.
A1	6-10+"	Black (10YR 2/1) silt loam; very high in organic matter; abundant fine and medium root systems.

\*Colors by Munsell notation taken for moist soil under field conditions.

### SOIL MOISTURE

Percent soil moisture is a ratio of the water weight times 100 percent to the weight of the dry mass of soil material. Many investigators have measured soil humidity since this more accurately describes the available free water. Soil humidity is a measurement of the vapor pressure of the water contained in the soil. It takes into account many of the soil variables such as aggregate composition, texture, structure, and the amount of organic matter which affect the availability of the soil moisture for evaporation.

There is no simple method for determining the humidity of a soil sample. Consequently, during the study the gravimetric process was employed for determining percent moisture content for field soil samples. The soil samples were sealed immediately after collection to avoid loss of moisture from the cans. Later in the soil laboratory, the samples were weighed wet, then oven dried, and finally weighed dry.

The soil samples were collected from the two-inch depth soil profile level. Care was exercised to avoid including roots, pebbles, and other extraneous material which would give erroneous soil moisture measurements. It was considered important to sample the soil moisture within the top horizon since this is the major source of water for evaporation during a particular twenty-four hour period. Most of the roots for meadow grass species are located within the top six inches of soil. Hence, transpiration from the grass will be dependent upon the available soil moisture from this top soil layer. Chudnovskii (1948) and others have indicated that soil moisture is the most critical

factor in removing heat from the soil surface. Water is active in providing a medium through which conduction of heat can occur from the surface into the soil sink. Evaporation of water removes enormous amounts of heat. Chudnovskii discusses other factors contributing to the surface soil temperature. Some of these are: amount of surface to surface area contact between soil particles, soil surface albedo, the soil skeleton shape; however, soil moisture far outweighs the combined effect of these other factors.

Sites III and VII maintained surface seepage and slow moving surface water respectively; hence they were classed as semi-swamp and swamp sites in that order. The percent soil moisture was sampled for the other sites as described except for two days for which no samples were taken. Time was a critical factor on these two days and conditions had not varied significantly from the previous soil moisture sampling periods.

Table 5 lists the percent moisture content measured at the two-inch level for each site. Along with this in parenthesis is a ranking of relative moisture content from wet to dry.

TABLE 5. PERCENT MOISTURE CONTENT FOR EACH SITE MEASURED AT THE TWO-INCH LEVEL

Date (1965)	Sites						
	I	II	III	IV	V	VI	VII
10-9	**	**	**	**	**	**	**
10-12	28%(6)	111%(4)	SS*(2)	26%(7)	79%(5)	200%(3)	Swamp(1)
10-16	63%(6)	123%(4)	SS (2)	35%(7)	78%(5)	217%(3)	Swamp(1)
10-23	29%(6)	51%(5)	SS (2)	19%(7)	52%(4)	102%(3)	Swamp(1)
10-26	**	**	**	**	**	**	**

\*SS is equivalent to semi-swamp.

\*\*No data collected on this date. The moisture contents are assumed to be similar to the next closest sampling period.

RADIATION-TEMPERATURE MEASUREMENTS

The Stoll-Hardy HL<sup>4</sup> Radiometer was an integral part of the study and proved to be an ideal instrument for collecting field R-T data. Radiometric temperature measurements can be made with the instrument to within  $\pm 0.1$  °C accuracy. The radiometer consists of a temperature-sensing head, reference ambient temperature body, amplifier, meter, range selector circuit, and power supply all contained in an oak carrying case (Figure 7). The carrying case was mounted in a canvas container with shoulder straps to facilitate rapid R-T measurements under field conditions (Figure 8). The R-T measurements are based on the Stefan-Boltzmann law for blackbody radiation (page 6).

To make a R-T measurement, the radiometer head is inserted in the reference ambient temperature block and the meter adjusted to zero. Then the head is removed from the block and directed toward a target. The radiometer head has a 20 degree acceptance angle. When the 20 degree cone is projected from the hand held position approximately four feet above the ground, the diameter of the circle sampled on the ground is about 18 inches. The radiometer head contains four thermistor infrared sensing elements; two of the elements are exposed to infrared radiation from a target and this is compared to the radiation from the sensing head itself by the other two thermistors. The deviation in surface R-T of the target from that of the ambient temperature block which is at the same temperature as the sensing head, is read from the preselected 10, 30, or 100 degree centigrade range scales. The R-T for the surface of the target is the meter reading added to or subtracted from the thermometer reading for the temperature of the

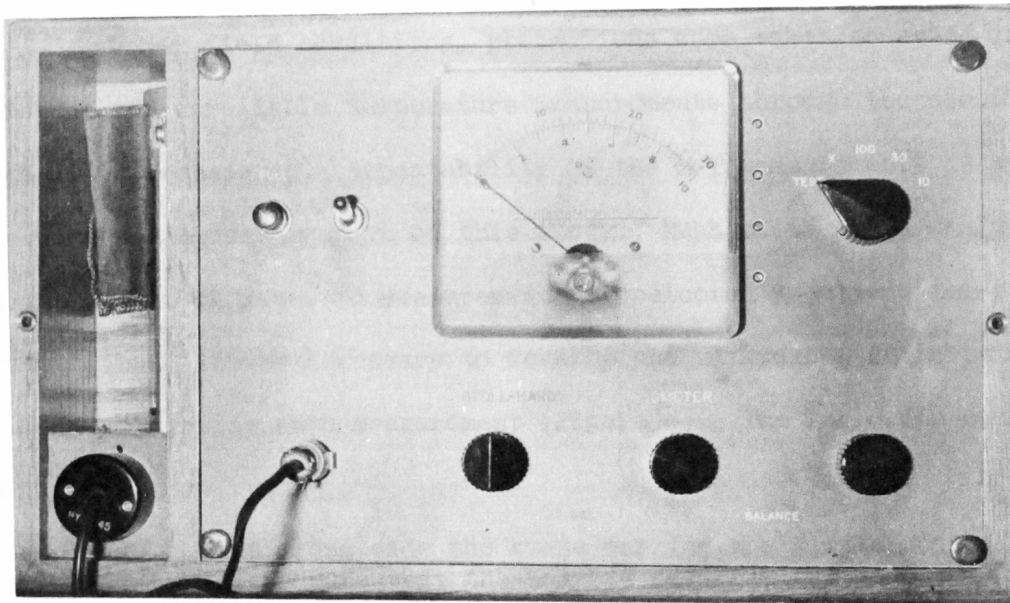


Figure 7. Stoll-Hardy HL4 Radiometer which was used for collecting R-T measurements. The sensing head located in the ambient temperature block is in the lower left hand corner of the instrument.



Figure 8. This shows the sampling procedure which was employed throughout the study. The radiometer was carried in the canvas case with shoulder straps. Much of the time a tape recorder was used for recording the data.

reference ambient temperature block.

Under field conditions, precautions were taken to avoid inconsistent and unreliable temperature measurements through the use of good measuring techniques. Repeatability of the R-T measurements is an important and necessary part of this study. Much of the data analysis is dependent on repeated measurements of selected locations for each site. Thus, it was necessary to develop and maintain a definite procedure for making each measurement (Figure 8). The following outlines this procedure:

- (1) Step along side the stake marking the sample point making sure that the body is square with the plot axis.
- (2) Adjust the meter to zero and read the ambient temperature thermometer.
- (3) Extend the left arm at a right angle to the north-south oriented plot with the radiometer head pointed vertically downward.
- (4) Read the R-T measurement which is either above or below ambient and replace the radiometer head in the ambient temperature block.
- (5) Proceed to the next sample point and repeat.

An example of the form used for recording the R-T measurements and other control information is included on the following page (Figure 9). On this form various control data were recorded for each site such as cloud cover and type, wind velocity, time of R-T measurement, sky R-T, and sun R-T. Part of the time this form was completed in the field by a second research aid concurrently with collection of the data. However, when working independently, it was necessary to record the data with a tape recorder and transcribe the information at a later date to the data forms. Both methods worked satisfactorily.



SITE #						SITE #									
COMMENTS	TIME	SAMP	AMB.	R.RDG.	R-T	COMMENTS	TIME	SAMP	AMB.	R.RDG.	R-T				
		1						1							
		2						2							
		3						3							
		4						4							
		5						5							
		6						6							
		7						7							
		8						8							
		9						9							
		10						10							
		11						11							
		12						12							
$\bar{Y} =$		$\Sigma Y =$		$\Sigma Y^2 =$		$(\Sigma Y)^2 =$		$\bar{Y} =$		$\Sigma Y =$		$\Sigma Y^2 =$		$(\Sigma Y)^2 =$	

SITE #						SITE #									
COMMENTS	TIME	SAMP	AMB.	R.RDG.	R-T	COMMENTS	TIME	SAMP	AMB.	R.RDG.	R-T				
		1						1							
		2						2							
		3						3							
		4						4							
		5						5							
		6						6							
		7						7							
		8						8							
		9						9							
		10						10							
		11						11							
		12						12							
$\bar{Y} =$		$\Sigma Y =$		$\Sigma Y^2 =$		$(\Sigma Y)^2 =$		$\bar{Y} =$		$\Sigma Y =$		$\Sigma Y^2 =$		$(\Sigma Y)^2 =$	

SITE #						SITE #									
COMMENTS	TIME	SAMP	AMB.	R.RDG.	R-T	COMMENTS	TIME	SAMP	AMB.	R.RDG.	R-T				
		1						1							
		2						2							
		3						3							
		4						4							
		5						5							
		6						6							
		7						7							
		8						8							
		9						9							
		10						10							
		11						11							
		12						12							
$\bar{Y} =$		$\Sigma Y =$		$\Sigma Y^2 =$		$(\Sigma Y)^2 =$		$\bar{Y} =$		$\Sigma Y =$		$\Sigma Y^2 =$		$(\Sigma Y)^2 =$	

FEATURE		1	2	3	4	5	6	7	8	9	10	
	R.RDG.											$\Sigma Y =$
TIME:	AMB.											$N =$
	R-T											$\bar{Y} =$
	R.RDG.											$\Sigma Y =$
TIME:	AMB.											$N =$
	R-T											$\bar{Y} =$

Figure 9. Form for recording field R-T data.

Sky and sun R-T measurements were taken by pointing the radiometer head vertically upward and directly at the sun respectively. These measurements provide information about the intensity of incoming insolation. Some useful information was acquired from this data regarding diurnal and meteorological induced variations in insolation receipt. Comparisons between daily receipt of insolation are also possible from this data (Table 14). There are certain filter problems which are discussed in the appendix regarding the sky and sun R-T data (page 64). Although, as explained in the appendix, the sky and sun R-T readings are considered to be reliable measurements of relative atmospheric transparency since the radiometer head was consistently pointed either vertically upward or directly at the sun.

A hygrothermograph was operated continuously and this provided the air temperature and humidity control information. The wind velocity was measured three times on each site during each sample period. This information is summarized on pages 67 to 70 by Tables 11 to 14.

#### IV. DATA ANALYSIS

Soil moisture is an important determinant of surface temperature for a given site. There are other factors which tend to obscure the soil moisture relationship. For example, meteorological conditions, aspect and slope, variations in soil parameters, vegetation differences, and others are important determining factors in the surface R-T expression for a given site and at a given time. One of the purposes of analyzing the R-T data is to attempt an evaluation of the relative importance of some of the mentioned variables and determine their influence on image recognition of moisture sites on IR imagery.

Small differences in soil moisture as related to surface R-T are difficult to analyze conclusively because of the number of other factors which play secondary roles in the surface R-T expression. There are significant differences in R-T, however, resulting from gross differences in moisture content. An analysis of variance procedure was employed in determining the significance of temperature differences for the seven sites. From this analysis and other considerations the time and meteorological conditions most conducive to high image production of moisture differences were deduced.

Throughout this study, the data were analyzed by rapid data processing techniques utilizing an IBM 1620 computer and a card sorting machine both located on the University of Montana campus. The author wrote the programs necessary for analyzing the data and operated the computer. The Fortran II computer programs were checked by working through the procedures manually.

RADIATION-TEMPERATURE GRAPHS

The R-T measurements used in this data analysis were collected over five different days during October, 1965 and the R-T means by site were plotted over time (Figures 36 to 40 in the appendix). Two of the R-T collection days extended over a twenty-four hour period while the others ran from morning to around midnight. Observations and analysis of these graphs indicate that the greatest differences in R-T between sites occur shortly past 1200 or approximately at the true solar noon for the Lubrecht area. The graphs indicate that R-T drops off sharply and many cross overs occur between 1600 and 1700 each day. Sunset varied between 1630 and 1645 and complete sunshine covered all the plots between 0730 and 0745 for this particular location and season. All features are approaching an apparent common R-T during the early morning hours before sunrise. The influence of wind and variable cloud cover causes erratic curve patterns as is illustrated by Figure 37. The steepest sloping curves occurred on the afternoon of October 16 when sky conditions were clear and site moisture conditions were not greatly influenced by previous precipitation.

Observations for the mean R-T values plotted over time in Figures 36 to 40 indicate variations resulting from a past history of precipitation. Precipitation occurred between October 12 and 16, as well as between October 16 and 23. There is a strong indication from the weather data (Table 14) that October 16 may have been the clearest day; but, due to the surface moisture conditions for the sites, the variation expected did not materialize. On October 23, the weather conditions were also quite clear and the time lapse since the last

precipitation was three days. This may explain the reason for more surface R-T variation due to slope and aspect on October 23 as will be explained later. The sites were poorly ranked according to soil moisture as correlated to the ranking of surface R-T on October 16 but the correlation is better on October 23. The soil moisture is less for the top soil horizons on 23 than on October 16. There is an indication that the surface soil moisture at or near saturation resulting from recent precipitation may result in more rapid evaporation from the sites with less vegetation and more porous soils. This would seemingly decrease the surface R-T disproportionately.

Other surface R-T anomalies which may be related to a history of precipitation occurrence include the reversal of the R-T means for the reservoir and stream. There is a possibility that due to the warm surface temperatures of the collecting basin for the stream and because additional surface runoff occurred due to the precipitation, more warm water was discharged through the stream. Thus the reservoir, due to its large volume in comparison to its surface area and in comparison to the volume of incoming warm water, maintained colder surface temperatures than the stream during and following the periods of precipitation.

The surface R-T for the boulder was always sampled on the south exposure. Thus high surface temperatures were recorded since the surface of the boulder was exposed to direct solar insolation. Other factors resulting in high surface R-T values for the boulder include its poor conductivity rate and the large volumetric heat capacity resulting from the continuity of the rock mass. These factors result in more re-radiation during periods of peak insolation receipt and a higher rate of

emission for a prolonged time during the night.

#### DETERMINATION OF THE BEST IMAGERY COLLECTING TIME

The R-T measurements for the seven sites were collected over a period of time, usually taking less than twenty minutes to sample the seven sites. Because of the slope of the curves during the twenty minute time periods, it was necessary to adjust each R-T reading by a determined correction value so that the site averages were moved along their respective curves to one point in time. A more detailed description of the procedure used for adjusting the means is described in the appendix on page 89. The expanded graphs showing the peak R-T periods (Figures 42 to 46) from which the correction factors were extracted are shown in the appendix.

Each of the 13 R-T sampling periods between 1100 and 1500 for the seven sites were adjusted to a mean time for the particular sampling period and these times are represented by the 13 vertical lines on the expanded graphs, Figures 42 to 46. The data for these periods were analyzed by analysis of variance and the results are listed in Table 7 regarding the significance between means. An example of the procedure used in analyzing the significance between means is illustrated in Table 6 using the data for the sampling period considered to be most ideal for collecting IR imagery which would probably illustrate the greatest tone contrasts between the selected moisture sites. Duncan's multiple range test was used for analyzing the ranked means and this procedure was repeated for each of the 13 sample periods. This test demonstrates the level of confidence which can be placed in the differences between one mean and all the other ranked means being considered.

TABLE 6. MASTER TABLE FOR THE ANALYSIS OF VARIANCE

Date: 10-12-1965 Time: 1110

DF	Source of variation	N.S.S.	M.S.	F	Sig.
	$C.F. = \frac{(Y)^2}{84} = 35,584.46$				
83	Total = $Y^2 - C.F.$	611.78			
6	Site total = $(Y_I)^2 + (Y_{II})^2 + \dots + (Y_{VII})^2 / 12 - C.F.$	513.84	85.94	67	**
77	Error within sites by subtraction	97.94	1.2719		

Significance of difference between means by  
Duncan's multiple range test.

$$S.M. = \sqrt{\text{Error mean Sq.}/12} = \sqrt{1.2719/12} = .3255$$

Value of P	2	3	4	5	6	7
F table values	2.83	2.98	3.08	3.14	3.20	3.24
Minimum difference between means	.92	.97	1.01	1.02	1.04	1.06

P = The number of ranked means that the significance is being tested across.

Table 7 gives the sample periods from 1000 to 1500 for each of the five data collecting days. This table shows the adjusted means ranked from low to high surface R-T; the site number is listed above each mean, the number in parenthesis shows the relative moisture content ranking from wet to dry, a ranking for the top imagery col-

lecting periods is indicated in the right margin along with the range between high and low R-T, and any site means underlined by the same line are shown as being non-significant at the 95 percent level of confidence. The ranking for the best imagery collecting periods as shown by Table 7 was based on the following criteria: (1) the moisture sites should be ranked according to soil moisture when ranked by surface R-T; (2) sites I and IV should be significantly different from the other sites, sites II, V, and VI should be significantly different from the other sites, and sites III and VII different also; and (3) the range in surface R-T between the low and high moisture sites should be large.

The expanded graph in the appendix, Figure 43, shows that the period from 1100 to 1230 on October 12, 1965 exhibits wide differences in R-T for the seven perfectly ranked moisture sites. The meteorological conditions preceding this period were important factors in creating the large differences in surface R-T. There had been no recorded rain since late September, thus the sites were evaporating only from stored sources of water. It is quite likely that potential soil moisture as a limiting site quality factor is expressed more by the surface R-T for a given site under these conditions than it is following a period of precipitation when the surface pores are near saturation. The minimum relative humidity had ranged between 20 and 45 percent for each day since the first of October.

The influence of wind on imagery quality of water related features is not understood completely. Gates (1963) has determined experimentally that during the daylight hours transpiration plays an



TABLE 7. SIGNIFICANCE OF SITE MEANS

Date	Time	Ranked Means of Sites <sup>1</sup>	A <sup>2</sup>	F <sup>3</sup>	Temp. Range
9	1152	7 (1) 3 (2) 2 (4) 6 (3) 5 (5) 1 (6) 4 (7) 20.89 22.93 23.72 <u>24.39</u> <u>24.73</u> 25.87 26.74	2	78	5.8
9	1354	7 (1) 3 (2) 2 (4) 6 (3) 5 (5) 1 (6) 4 (7) 22.70 24.10 24.93 <u>26.02</u> <u>26.16</u> <u>26.30</u> 27.23	5	23	4.5
12	1110	7 (1) 3 (2) 6 (3) 2 (4) 5 (5) 1 (6) 4 (7) 16.11 18.34 <u>20.47</u> <u>20.89</u> <u>21.52</u> 22.52 24.20	1	67	8.1
12	1220	7 (1) 3 (2) 2 (4) 6 (3) 5 (5) 1 (6) 4 (7) 18.70 21.13 <u>22.70</u> <u>23.11</u> <u>23.59</u> <u>25.01</u> 25.10	3	75	6.4
12	1320	7 (1) 3 (2) 2 (4) 4 (7) 5 (5) 1 (6) 6 (3) 20.08 21.53 <u>22.75</u> <u>23.01</u> <u>23.03</u> <u>23.08</u> 24.40		28	4.3
16	1240	7 (1) 3 (2) 6 (3) 1 (6) 2 (4) 5 (5) 4 (7) 12.94 14.70 <u>18.33</u> <u>18.54</u> <u>19.05</u> <u>19.84</u> 20.06		66	7.1
16	1350	7 (1) 3 (2) 1 (6) 2 (4) 6 (3) 5 (5) 4 (7) 13.70 15.32 <u>18.23</u> <u>18.76</u> <u>19.00</u> <u>19.22</u> 19.92		71	6.2
23	1210	7 (1) 3 (2) 6 (3) 2 (5) 1 (6) 5 (4) 4 (7) 15.47 18.07 <u>20.89</u> <u>21.25</u> <u>21.45</u> <u>22.30</u> 22.95		39	7.5
23	1340	7 (1) 3 (2) 6 (3) 2 (5) 5 (4) 1 (6) 4 (7) 19.30 20.98 <u>23.33</u> <u>23.60</u> <u>24.41</u> 23.80 25.45	4	42	6.2
23	1520	7 (1) 3 (2) 2 (5) 6 (3) 5 (4) 1 (6) 4 (7) 17.15 <u>19.37</u> <u>20.30</u> <u>21.15</u> <u>21.29</u> <u>21.61</u> <u>22.28</u>		7	5.1
26	1216	7 (1) 3 (2) 6 (3) 2 (5) 5 (4) 1 (6) 4 (7) 15.31 17.26 <u>20.40</u> <u>21.02</u> <u>21.40</u> <u>22.00</u> 23.21	6	57	7.9
26	1330	7 (1) 3 (2) 6 (3) 2 (5) 1 (6) 5 (4) 4 (7) 18.50 20.47 <u>23.01</u> <u>23.29</u> <u>23.88</u> 24.15 25.15		51	6.6
26	1500	7 (1) 3 (2) 2 (5) 6 (3) 5 (4) 1 (6) 4 (7) 18.08 19.51 <u>20.81</u> <u>21.33</u> <u>21.50</u> <u>21.88</u> 22.43		23	4.4

<sup>1</sup>Any two means or more not underlined by the same line are significantly different at the 95% level of confidence.

<sup>2</sup>Ranking of the best IR imagery collecting periods.

<sup>3</sup>Analysis of variance is significant at the 95% level of confidence when the F ratio exceeds 3.04.

important role in determining the surface temperature of leaf structures. But he indicates that transpiration may prove to be a secondary effect if the forced convection (wind) increases to 2-3 miles per hour. The recorded wind was 3-4 miles per hour for the best imagery collecting period and the wind increased to 5-6 miles per hour for the third best imagery collecting time. Air ventilation across a water surface increases the amount of evaporation which would tend to increase the surface R-T differences between sites. But there may be a horizontal transfer of heat from one site to an adjacent site resulting from the air movement. These factors may counteract one another. Air temperature is thought to be only remotely related to the expression of relative differences in R-T between sites. Air temperature or sensible heat is significantly affected by the transfer of heat through the air-soil interface and subsequent free and forced convection in the atmosphere.

All indications from the collected data are that clear weather is necessary to build up the surface R-T differences. The five graphs, Figures 42 to 46, back this conclusion, since they show the greatest differences in R-T on cloud free days. These data are somewhat limited for this evaluation, however, since the common weather conditions were not adequately sampled. For example, Geiger (1957) states that less surface R-T variation resulting from small slope and aspect differences occurs on overcast days. It is possible that soil moisture induced surface R-T may be expressed more clearly and that the IR imagery interpreter, when mapping soil moisture sites, may find it unnecessary to consider slope and aspect conditions as much under continuous cloud cover conditions.

VARIATION WITHIN SITES RESULTING FROM GRASS HEIGHT

When conducting an experiment under wildland conditions, one can expect to encounter variables which are difficult or nearly impossible to control. The outdoor laboratory also provides a place for tests under natural environmental conditions, where observations can be made in the "real world" about conditions which actually exist. One of the objectives of this study was to determine some of the variables and their effect on obscuring soil moisture induced surface R-T and possibly to determine the expected variation in R-T resulting from these variables.

In the field an effort was made to determine the difference between paired plots; one plot covered with natural grass vegetation and its clipped grass counterpart. Other factors including moisture content were constant between the paired plots. Examples of the clipped sites are shown by Figures 31 to 35. Site I is similar to site IV and site II is similar to site V. It is not normal to find sites clipped as closely as these were under wildland grazing conditions.

A regression analysis procedure failed to show any definite significant relationship and the literature did not reveal any functional correspondence describing the variation in R-T due to different grass heights. However, for the peak insolation period, it can be conclusively demonstrated by Figure 10 that the clipped sites are about one full degree centigrade warmer than the unclipped. At night, there is a definite trend toward the clipped sites maintaining a higher level of energy emission for a longer period than the natural grass sites. This may be a result of increased absorption and less

reflection from the clipped sites. The night phenomena is especially noticeable for site III where the grass is quite tall and it is cured out completely. Immediately following sundown, the grass cools very rapidly on site III, but the clipped region maintains an elevated temperature nearly three degrees centigrade warmer. Cured dry grass is thought to reflect considerable insolation during the day and at night may blanket the ground holding heat in while radiating very rapidly the heat stored in the grass. The grass, due to its low volume to surface area ratio, cools very rapidly under radiation cooling conditions.

On each of the 12 sample points for each site an average grass height was measured (Table 2). Linear regression analysis was applied to sites III, V, and VII to determine if surface R-T and these average grass height measurements are correlated. The other sites were ignored at this stage because of large variations in aspect and slope between sample points. But for sites III, V, and VII no noticeable differences in slope and aspect were observed between R-T sample points; the only major variation apparent being that due to differences in grass height. Sites III and V failed to correlate either negatively or positively with any reliability. Site VII showed an average regression coefficient for grass height of 0.35 and an average correlation between grass height and surface R-T of 0.50. Upon analysis of the sample point photographs, it was observed that for site VII grass height is related to percent grass cover and thus R-T is not correlated directly to grass height (Figures 11 and 12). These two photographs are examples of the general relationship observed for the other sample points. The grass height measurements

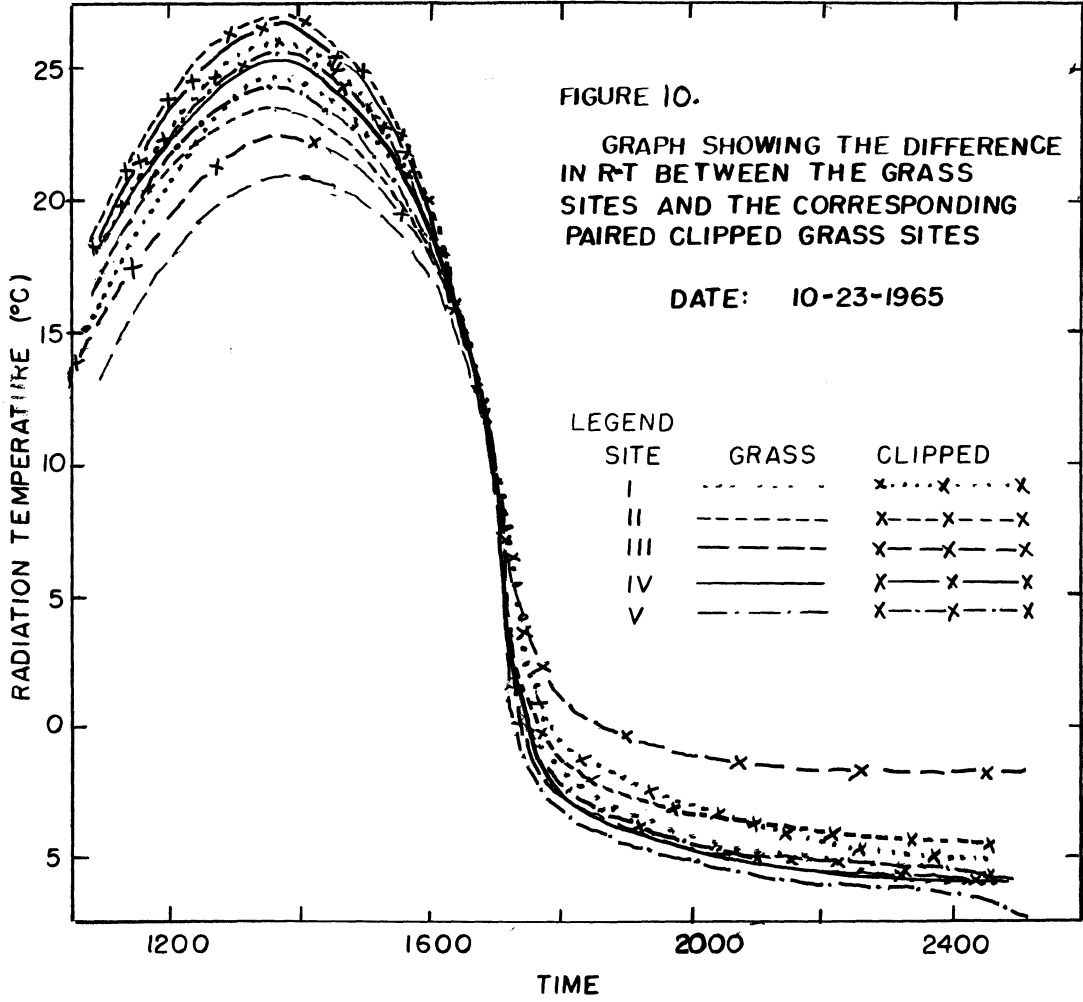




Figure 11. Photograph of sample point 1 on site VII showing the general correlation between grass height and density of the sedge vegetation.



Figure 12. Photograph of sample point 11 on site VII showing the general correlation between grass height and density of the sedge vegetation on this site.

are apparently not extremely descriptive of the grass variation induced differences in surface R-T. However, a multiple regression analysis determining the effect of grass height and microslope and aspect on surface R-T will be discussed later.

#### VARIATION WITHIN SITES RESULTING FROM MICROSLOPE AND ASPECT DIFFERENCES

Aspect and slope combined account for a high percentage of the variation between surface R-T values for the sample points on each site. This is especially true for sites I, II, and IV since these are the sites with the greatest variations in slope and aspect. The amount of variation in surface R-T due to microrelief phenomena is probably a complex function involving time of day, meteorological conditions, and season of year. The effect of diurnal variation and meteorological conditions will be discussed. The data were collected during the month of October, hence no knowledge regarding seasonal variation can be extracted from the data. A preliminary analysis using Spearman's rank correlation indicated that there is a strong relationship between slope and aspect variation and surface R-T. Angles of insolation incidence as a function of time for solar radiation receipt on each sample point were calculated by a method described in the appendix, pages 71 to 76.

The results for the linear regression analysis can best be demonstrated by a graphical representation of the best-fit regression equations showing surface R-T as a function of angle of insolation incidence. These functions for each sample period on site I for each of the five days between 0900 and 1500 hours are graphically shown by Figures 47 to 51. The linear regression lines for the hour period from

1300 to 1400 for each of the five days for sites I and IV are shown by Figures 13 and 14 respectively. The latter two figures show regression lines which were adjusted to the same mean and are balanced about this mean value by the product moment regression method. The regression constant, the independent regression coefficients, the correlation values, the wind, and the cloud cover for each of the regression lines are listed in Table 8.

The specific slopes for different regression equations under varying atmospheric conditions indicate the relative influence of different levels of atmospheric disturbance. With no clouds present in the atmosphere the regression lines have a steeper slope than with a cloud cover present. This is well illustrated on October 12 (Figure 48) when the regression line had a steep slope during the clear morning hours and later, after 1300, a cloud cover moved in resulting in more shallow sloped regression lines. The flat curves are a result of less variation due to the slope effect between sample points. In other words, a greater percentage of indirect insolation is incident on each plot point in near equal amounts regardless of slope and aspect. On October 23 the regression lines have the steepest slopes and from an examination of the weather data (Tables 13 and 14) this appears to be one of the days with the highest transparency to solar radiation. October 16 had very clear atmospheric conditions; however, there is an apparent evening out of slope and aspect induced R-T variation on this date due to recent precipitation.

The regression lines for 1300 to 1400 hours for sites I and IV (Figures 13 and 14) confirm the slope relationship for the various atmospheric conditions prevailing on each of the five days. The slopes



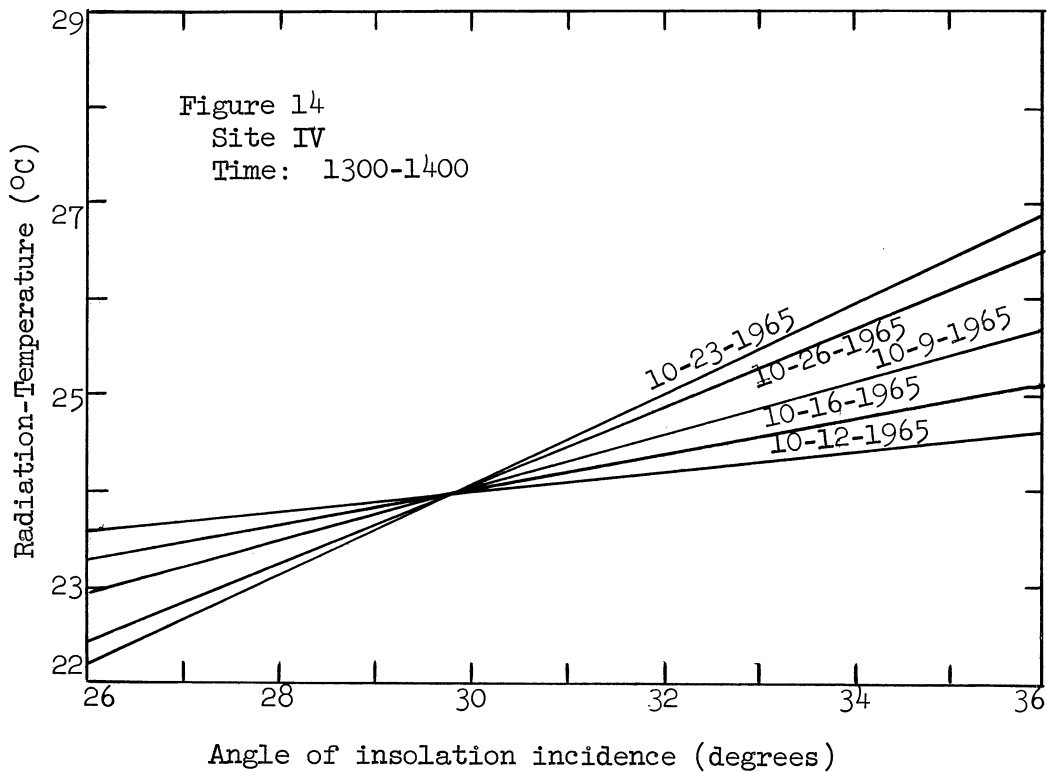
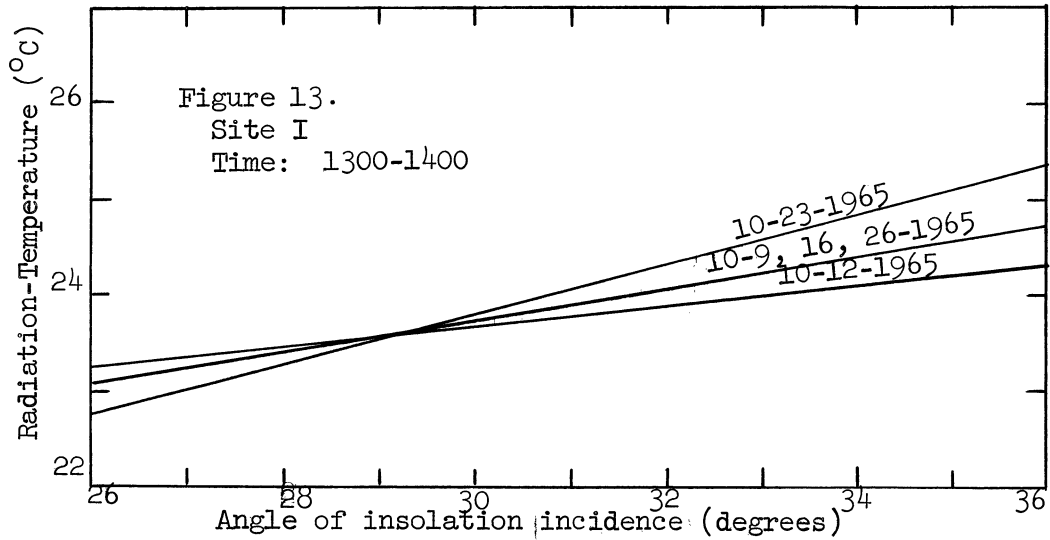
TABLE 8. EQUATIONS FOR REGRESSION CURVES (FIGURES 47 TO 51)

Date	Time	Site	Wind (MPH)	Cloud Cover*	Constant	Slope	Correlation Coefficient
9	1001	I	0	01	15.01	.1352	.63
9	1130	I	3-4	01	19.98	.1772	.69
9	1340	I	7-8	01	21.88	.1622	.58
12	1001	I	1-2	03	10.88	.1848	.82
12	1058	I	1-2	01	19.26	.0935	.32
12	1204	I	5-6	01	21.79	.1062	.31
12	1309	I	5-6	04	20.73	.1048	.46
12	1402	I	3-4	06	19.84	.0026	.01
16	1104	I	5-6	01	11.36	.1315	.51
16	1230	I	7-8	01	13.11	.1723	.62
16	1346	I	7-8	01	13.81	.1553	.43
16	1453	I	5-6	01	8.93	.3175	.63
23	1054	I	1-2	01	9.37	.2674	.75
23	1156	I	1-2	01	13.46	.2484	.58
23	1323	I	0	01	17.22	.2571	.79
26	1008	I	0	01	11.48	.0428	.13
26	1158	I	1-2	02	15.08	.2033	.68
26	1310	I	0	02	19.06	.1690	.59
26	1449	I	0	02	17.54	.1907	.69
12	1309	I	5-6	04	20.73	.1048	.46
9	1340	I	7-8	01	21.88	.1622	.58
16	1346	I	7-8	01	13.81	.1553	.43
26	1310	I	0	02	19.06	.1690	.59
23	1323	I	0	01	17.22	.2571	.79
12	1317	IV	5-6	05	20.25	.0959	.42
16	1355	IV	5-6	01	14.28	.1794	.72
9	1353	IV	7-8	01	19.48	.2604	.91
26	1326	IV	1-2	02	13.00	.4082	.94
23	1335	IV	1-2	01	11.85	.4566	.96
12	1309	II	5-6	05	20.18	.0885	.37
9	1344	II	7-8	01	21.72	.1096	.51
23	1327	II	1-2	01	18.08	.1830	.89
26	1315	II	0	02	16.87	.2093	.87
16	1349	II	3-4	01	11.15	.2522	.66

\*Cloud Cover Legend

- 01 Clear
- 02 Very thin cirrus
- 03 Scattered cirrus
- 04 High partial overcast
- 05 Overcast
- 06 Thin alostratus

Figures 13 and 14. Regression lines for five days. (Radiation-temperature as a function of angle of insolation incidence).



for the regression lines can be divided into three classes. A steep sloping line for October 23 demonstrates the effect of clear weather. A flat curve for October 12 shows the influence of cloudy weather conditions. The intermediate slopes represent average atmospheric transparency conditions with the effect of precipitation which preceded October 16 acting to dampen the amount of R-T variation on sites I and IV normally resulting from differences in slope and aspect. On site II for October 16 there is evidence which indicates that the precipitation had little influence on the slope and aspect induced variation (Table 8). This may be due to the normal high surface moisture content noted for this site.

The high correlation values corresponding to the regression slope values indicate a high correspondence between angle of insolation incidence and surface R-T under a specified set of prevailing weather conditions. Providing a site contains differences in slope and aspect will determine to a large extent the size of the standard deviation and standard error of the mean for that site. The magnitude of the standard deviation, then, is dependent on the steepness of the regression line and how highly correlated surface R-T is to insolation angle of incidence.

#### RADIATION-TEMPERATURE AS INFLUENCED BY MAJOR SLOPE DIFFERENCES

One of the major limiting factors in using IR imagery for mapping soil moisture may be the false tone representation on the imagery corresponding to a surface R-T which is a result of small changes in slope from one side of a small depression to the other or

from a south exposure of a knoll to the north slope. The flux of heat in a horizontal direction (Tanner, 1960) between warm surfaces and cold surfaces tends to even out the effect of slope and aspect as well as other variation between sites or sample points within a site resulting from ecological and terrain conditions. Variation in surface R-T within a site correlated to small areas of different slopes and aspects are thought to be affected more by the transfer of heat through the soil and air in a horizontal direction than are variations in R-T resulting from larger areas of the same feature with the same variables. Therefore, an inference of the minimum difference in surface R-T which might be expected for two sites of the same moisture content but differing in aspect might be accomplished from the data obtained during this study. The angle of incidence at 1330 for each day was approximately 31 degrees from the horizontal. Considering a 5 degree north slope and a 5 degree south slope, the following differences which might be expected in surface R-T were inferred using Figures 13 and 14.

TABLE 9. DIFFERENCES IN SURFACE R-T WHICH MAY RESULT BETWEEN NORTH AND SOUTH FACING SLOPES

Date	Time	Angle of insolation incidence (Degrees)		Expected difference in surface R-T (°C)	
		north slope	south slope	Site I	Site IV
9	1330	26	36	1.5	2.5
12	1330	26	36	1.0	1.0
16	1330	26	36	1.5	1.5
23	1330	26	36	2.5	4.5
26	1330	26	36	1.5	4.0

From Table 9 there is an indication that during periods of cloudy weather the least differences in surface R-T which are a result

of different aspects occur. There is a possibility that the best IR imagery may be attained under a continuous cloud cover providing sufficient solar energy is received by the moisture sites to build up the necessary gradient of surface R-T differences necessary for producing tone contrasts on the IR imagery. The effect of a discontinuous cloud cover is definitely not desirable since unequal insolation receipt may occur for two sites of otherwise equal conditions. The effect of slope in determining surface R-T is thought to be less pronounced during the summer solstice when the solar energy is incident at the highest angles. The effect of microrelief changes, however, is noted to be least just before sunset when the angle of incidence is lowest. It can be reasoned that at this time many features are cooling rapidly while others maintain a more continuous emission intensity, thus there are many crossovers between curves for individual sample points. This will be discussed in more detail later. It is felt that the effect of slope and aspect is an important consideration and warrants a more detailed study in the future.

THE COMBINED EFFECT OF ANGLE OF INSOLATION INCIDENCE AND GRASS HEIGHT ON SURFACE R-T.

An expression of both grass height and angle of insolation receipt by a two independent linear regression analysis plane was attempted. The regression coefficients and constants are listed by date and time in Table 10 for site I. Similar results were realized for sites II and IV; the only other two sites with both considerable variability in grass height and angle of insolation incidence between sample points. Student's T test is used here to determine the significance of

TABLE 10. MULTIPLE REGRESSION ANALYSIS OF 2 - INDEPENDENT VARIABLES  
(GRASS HEIGHT AND ANGLE OF INSOLATION INCIDENCE)

Date	Time	Regression constant	$B_{y1.2}$	$B_{y2.1}$	$T_{By1.2}$	$T_{By2.1}$	F Ratio	R
9	1001	13.3806	.1735	.4845	5.36*	4.36*	18.95*	.89
9	1130	18.9689	.1978	.3019	3.57	1.61	6.73	.77
9	1340	21.1597	.1721	.2960	2.59*	1.61	4.31	.69
12	1001	10.9815	.1826	-.0273	4.14*	-0.18	9.50*	.82
12	1058	16.9733	.1471	.6775	2.21	2.96*	5.47	.74
12	1204	19.7543	.1411	.6735	1.79	2.72*	4.51	.70
12	1304	20.1251	.1132	.2492	1.92	1.52	2.75	.61
12	1402	19.4019	.0019	.3083	0.02	1.80	1.62	.51
12	1457	16.0316	.0302	.1756	1.42	3.43*	6.94*	.77
16	1104	9.6707	.1657	.5026	2.91*	2.61*	6.23	.76
16	1230	13.9071	.1588	-.2615	2.39*	-1.26	4.26	.69
16	1346	14.9078	.1402	-.4504	1.50	-1.74	2.91	.62
16	1453	9.7827	.3188	-.6018	3.23*	-2.52*	8.36*	.80
23	1054	10.5889	.2389	-.3613	3.29*	-1.45	8.40*	.80
23	1156	14.7565	.2222	-.3843	1.98	-1.01	3.11	.63
23	1323	17.5660	.2524	-.1402	3.90*	-0.78	8.29*	.80
26	1008	8.1574	.1208	.9872	2.13	5.07*	13.20*	.86
26	1158	14.2749	.2195	.2379	3.09*	.99	4.82	.71
26	1310	18.7203	.1737	.1414	2.21	.65	2.55	.60
26	1449	17.2777	.1903	.1869	3.15*	1.28	5.82	.75

$$\hat{Y} = \text{Regression constant} + (\text{Angle of insolation incidence}) \\ (B_{y1.2}) + (\text{Grass height}) (B_{y2.1})$$

R = The multiple correlation coefficient.

$B_{y1.2}$  = The regression coefficient for the angle of isolation incidence.

$B_{y2.1}$  = The regression coefficient for grass height.

F ratio for significance at 95 percent level of confidence must be greater than 6.93.

T value for significance at 95 percent level of confidence must be greater than 2.23.

\* indicates significance of F ratio and T values at the 95 percent level of confidence.

each regression coefficient and the F ratio tests the overall significance of the regression plane. Partial correlation coefficients were calculated for each independent variable; however, the correlation between grass height and surface R-T was always low with the correlation between angle of insolation incidence and surface R-T comparing to those calculated in the single variable regression analysis. Table 10 shows that only in two cases were all three tests significant at the 95 percent level of confidence. In 11 out of 20 cases the regression coefficient for angle of insolation incidence was significant, and in 7 out of 20 cases the regression coefficient for grass height was significant. The important thing to be realized from these data is that certain trends seem to be expressed by the regression coefficients. There is a definite indication that precipitation has created a reversal in the slope of the regression plane along the grass height axis. This is shown by the negative regression coefficients for grass height on October 16 and 23. This would indicate that following precipitation the taller grass sample points were cooler. Under other conditions the grass appears to be proportional to surface R-T. No definite functional relationship has been described by this analysis for the relationship between grass height and angle of insolation incidence as they affect surface R-T either individually or in combination. However, the regression coefficients do indicate that there is likely some functional relationship if enough variables can be controlled or eliminated from the model statistically.

There are at least five reasons for the poor correlation of grass height with surface R-T: (1) The sample circles were 18 inches

in diameter. Thus, in any one circle the grass height varies considerably, especially for the taller grass heights. (2) A clump of grass may shade portions of the area of a given sample circle. This variation is difficult to account for since it changes with time. (3) The density of the grass varies between sample plots and within a sample plot which is thought to affect the surface R-T along with grass height. (4) The albedo varies between sample plots within a site and there is noticeable variation in percent albedo within some of the surface R-T sample circles. (5) There are other variables connected with the soil such as texture, compaction, amount of organic material near the surface, etc. which have not been accounted for in this analysis. Therefore, even though differences in grass height and in angle of insolation incidence are the more obvious sources of variation, the effect of these may not be significant in comparison to some of the undefined variables.

Possibly future experiments could test for grass height more advantageously by considering homogeneous lawn-type test sites where more control can be exercised. Such things as homogeneous grass stands; equal soil moisture between sites and between sample points within sites; similar meteorological conditions; or in other words, a controlled environment are considered necessary to clearly reveal this apparently subtle effect, grass height. The approach taken in this study for determining the influence of grass height on surface R-T using multiple regression analysis techniques is not efficient and a one variable more efficient regression analysis procedure could be employed providing a more highly controlled experimental design were used.



ANALYSIS OF SAMPLE POINT DEVIATES

There is additional information to be gained from the data by observing the deviates for the individual R-T values from their mean for various times during a twenty-four hour period. The standard deviation describes grossly how the components of a sample are distributed around the mean; however, diagrams of this deviate dispersion are especially useful since specific information is revealed regarding the dispersal for a given sample point. The deviates for site IV are illustrated by Figures 52 to 56. The major deviations occurred during the peak insolation periods and the minimum deviations for the R-T sample points occurred shortly before sundown. Later in the evening when radiation cooling was proceeding at a peak rate, a secondary maximum range of deviations developed. By midnight the variation was back to a low level with the transfer of heat horizontally by air conduction and convection being the suspected dominant forms of heat exchange.

The fundamental factors important to heat exchange can be applied in explaining deviation anomalies for the R-T sample points within a site. The points which are weak absorbers of heat may cool rapidly during periods of radiation cooling. In other words, the top layer of duff and soil may be acting in insulation which would reduce the rate at which energy is stored. The insulation layer may absorb the incoming radiation thus reaching a high surface temperature with negligible transfer of heat into the soil heat sink. However, because of the high surface temperature, the amount of radiation from this sample location would be large. Also, conduction of heat by the air

and subsequent convection would result in heat transfer away from the surface. On the other hand, incoming insolation may be directly reflected if the surface albedo is high. In this case, the surface would not reach a high temperature nor would heat energy storage be appreciable. Another sample point may readily absorb a large portion of the incident solar radiation and be a good conductor of the heat into the soil heat sink. For this example, it is possible that the sample point could have a negative deviate during the day and a positive deviate at night since it may maintain a longer period of heat emission at a higher rate than the other sample points.

It is interesting to observe the extreme deviate R-T sample points for a site and watch the positions of these points relative to the other sample points as time progresses. For all five days, points 3, 6, and 4 had extreme deviates and made some interesting changes in relative surface R-T in respect to the other sample points during the twenty-four hour periods (Figures 52 to 56). Plot point 3 had a positive deviate during the daylight hours and an extreme negative deviate position at night. Plot point 3 was south exposed as was point 6, however point 3 was light toned and only contained cured grass whereas point 6 contained some green grass (Figures 15 and 16). Probably point 6 absorbed more radiation during the day because of its apparently more moist, lower albedo condition than for point 3. Hence, at night these two points had opposite R-T deviations.

For October 12 (Figure 53) under variable cloudy skies, a reduction in the magnitude of the extreme deviates occurred. The deviate position for point 4 in relation to the other surface R-T de-

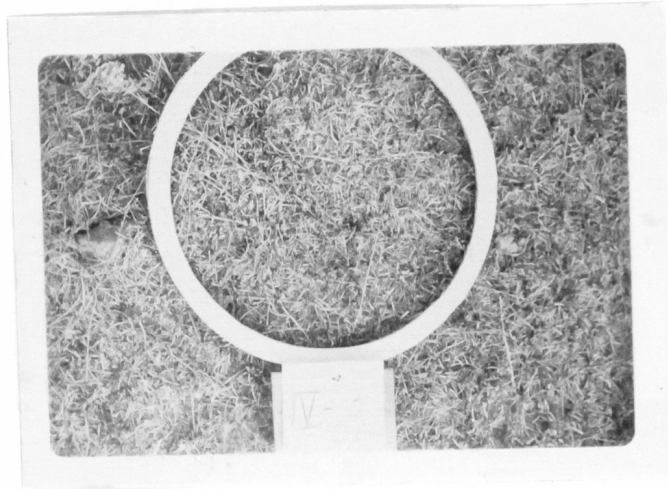


Figure 15. Photograph of sample point 3 on site IV showing the high albedo resulting from the cured grass on this point.

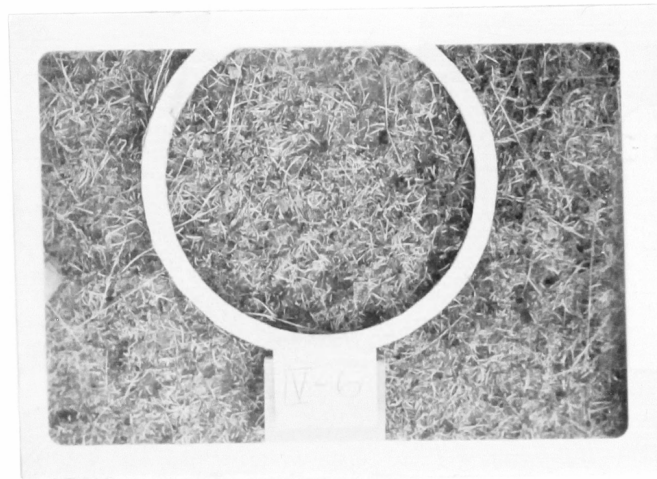


Figure 16. Photograph of sample point 6 on site IV shows the lower albedo which results in different heat transfer phenomena as compared to the above point in Figure 13.

viates is near zero under the existing sky cover conditions. This is considered to be a result primarily of more indirect insolation on sample point 4 than before, which results in a de-emphasis in the importance of slope and aspect as contributors to surface R-T variation. Standard deviation analysis revealed a reduction in the magnitude of deviations in R-T for individual sample points for all sites on October 12 under cloudy sky conditions.

## V. CONCLUSIONS

(1) From the literature and results of this study, there are indications that it is feasible to map major soil moisture differences on near level terrain using state-of-the-art infrared heat mapping scanner systems.

(2) The IR imagery most likely to show the greatest tone differences as related to soil moisture differences can best be imaged under the following conditions:

- (a) At least two weeks since the previous precipitation.
- (b) A cloudless day.
- (c) A day with little wind on the ground.
- (d) Between 1100 and 1300 hours.
- (e) Low humidity.
- (f) Stable air mass conditions.

(3) By clipping the grass on paired plots it was found that the clipped plots were about 1 degree centigrade warmer during the peak insolation period. The clipped plots maintained a higher temperature during the night also.

(4) Variation within sites is mainly a function of the micro-relief present on the site.

(5) Tall grass is thought to cool rapidly at night due to a low volume to surface area ratio.

(6) Small differences in grass height were not readily related to specific differences in surface R-T for this study.

(7) The effect of microrelief in determining surface R-T is

dependent on atmospheric conditions. Regression equations have a larger slope coefficient for clear days than for cloudy weather conditions.

(8) The multiple regression analysis indicates that there may be a relationship between grass height and surface R-T. Apparently the taller grass height sample points are warmer during periods of little past precipitation history. Negative regression coefficients for grass height were consistently obtained for the two days of R-T sample data for which precipitation was noted from one to three days before sampling. The taller grass height sample points were cooler for these two days than the shorter grass height points.

(9) Some problems in interpreting differences in tone related to soil moisture may result due to differences in surface R-T resulting from knolls and depressions in meadow areas. This could easily bias the interpreter's judgements regarding soil moisture classification from IR imagery.

(10) Maximum deviations between sample points occur near the time of maximum solar radiation receipt.

(11) Deviations about the mean temperature for a site decrease to a minimum before dusk and reach a secondary maximum deviation shortly after sundown. Then a gradual decrease in the amount of dispersion occurs until the following morning.

(12) Some plot points change from maxima during the day to minima surface R-T deviates for that site at night and the opposite also occurs. Other plot points remain in a positive or negative deviate position during the twenty-four hour period.

(13) Deviations decrease in cloudy weather and are an indication of relative transparency of the atmosphere.

## VI. BIBLIOGRAPHY

- Brenner, R. L. (1964), Geology of the Lubrecht Experimental Forest, Montana State University, Missoula, Montana. Unpublished.
- Buckman, H. O. and M. C. Brady (1959), The Nature and Properties of Soils, The Macmillan Company, New York.
- Cantrell, J. L. (1964), "Infrared Geology," Photogrammetric Engineering, Vol. 30, pp. 916-922.
- Carnahan, C. E. (1958), "Photogrammetry and Road Location in the United States Forest Service," Photogrammetric Engineering, Vol. 24, No. 3. pp. 404-410.
- Chudnovskii, A. F. (1948), Heat Transfer in the Soil, Israel Program for Scientific Translations, Jerusalem, 1962. Translated from Russian.
- Colwell, R. N. (1963), "Basic Matter and Energy Relationships Involved in Remote Reconnaissance," Photogrammetric Engineering, Vol. 19, No. 5., pp. 761-799.
- \_\_\_\_\_ (1964), "Aerial Photograph - A Valuable Sensor for the Scientists," American Scientist, Vol. 52, No. 1, pp. 16-49.
- \_\_\_\_\_ and D. L. Olson (1964), "Thermal Infrared Imagery and its use in Vegetation Analysis by Remote Aerial Reconnaissance," Proceedings of the Third Symposium on Remote Sensing of Environment. Report No. 4864-9-X, Institute of Science and Technology, The University of Michigan, Ann Arbor, Michigan, pp. 607-621.
- Fagerholm, P. O. (1959), "The Application of Photogrammetry to Land Use Planning," Photogrammetric Engineering, Vol. 25, No. 4, pp. 523-529.
- Fischer, W. A. (1964), "Infrared Surveys of Hawaiian Volcanoes," Science, Vol. 146, No. 3645, pp. 733-742.
- Gates, D. M. and C. M. Benedict (1963), "Convection Phenomena from Plants in Still Air," American Journal of Botany, Vol. 50, No. 5, pp. 563-573.
- \_\_\_\_\_ (1963), "The Energy Environment in which we live," American Scientist, Vol. 51, No. 3, pp. 327-347+.
- \_\_\_\_\_ (1964), "Characteristics of Soils and Vegetated Surfaces to Reflected and Emitted Radiation," Proceedings of the Third Symposium on Remote Sensing of Environment, Report No. 4864-9-X, Institute of Science and Technology, The University of Michigan, Ann Arbor, Michigan, pp. 573-600.

- Geiger, R. (1957), The Climate near the Ground, Harvard University Press, Cambridge, Mass. 494 pp.
- Gerlach, F. L. (1966), Unpublished research on soil heat transfer under controlled laboratory conditions and personal communication.
- Harris, D. E. (1964), "Terrain Mapping by Use of Infrared Radiation," Photogrammetric Engineering, Vol. 30, No. 1, pp. 134-139.
- Howe, R. H. L. (1960), "The Application of Aerial Photographic Interpretation to the Investigation of Hydrologic Problems," Photogrammetric Engineering, Vol. 26, No. 1, pp. 85-95.
- Lattman, L. H. (1963), "Geologic Interpretation of Airborne Imagery," Photogrammetric Engineering, Vol. 29, No. 1, pp. 83-87.
- Leonardo, E. S. (1964), "Capabilities and Limitations of Remote Sensors," Photogrammetric Engineering, Vol. 30, No. 6, pp. 1005-1010.
- Lowe, D. S., F. Polcyn and R. Shay (1964), "Multispectral Data Collection Program," Proceedings of the Third Symposium on Remote Sensing of Environment, Report No. 4864-9-X, Institute of Science and Technology, The University of Michigan, Ann Arbor, Michigan, pp. 667-680.
- Morgan, Joseph O. (1962), "Infrared Technology," Proceedings of the First Symposium on Remote Sensing of Environment, Contract No. 1224(44), Infrared Laboratory, Institute of Science and Technology, The University of Michigan, Ann Arbor, Michigan.
- \_\_\_\_\_ (1962), Proceedings of the Second Symposium on Remote Sensing of Environment, Contract No. 1224(44), Infrared Laboratory, Institute of Science and Technology, The University of Michigan, Ann Arbor, Michigan.
- \_\_\_\_\_ and V. L. Prentice (1966), "Third Symposium on Remote Sensing," Photogrammetric Engineering, Vol. 32, No. 1, pp. 98-108.
- Morris, M. S. (1966). Personal conversation and assistance in classifying vegetation.
- Nimlos, T. J. (1966). Personal conversation and assistance in describing the soils.
- Organick, E. I. (1963), A Fortran Primer, Addison-Wesley Publishing Company, Inc., Reading, Massachusetts.
- Ory, T. R. (1964), "Line-Scanning Reconnaissance Systems in Land Utilization and Terrain Study," Proceedings of the Third Symposium on Remote Sensing of Environment. Report No. 4864-9-X, Institute of Science and Technology, The University of Michigan, Ann Arbor, Michigan, pp. 393-398.



- Oshiver, A. H. and G. A. Berberian (1965), "Sensing Sea-Surface Temperature by Airborne IR," Geo. Marine Technology, Vol. 1, No. 4, pp. 22-26.
- Pierce, W. R. (Undated), An Introduction to Forest Statistics, University of Montana Press, Missoula, Montana, 64 pp.
- Pryor, W. T. (1964), "Highway Engineering Influences on Aerial Surveys," Photogrammetric Engineering, Vol. 30, No. 2, pp. 202-209.
- Snedecor, G. W. (1956), Statistical Methods, The Iowa State University Press, Ames, Iowa.
- Steel, R. G. D. and J. H. Torrie (1960), McGraw-Hill Book Co., Inc., New York, 481 pp.
- Steele, R. W. (1965), Lubrecht Experimental Forest Weather Data, Greenough Station 1965 and 9-Year Averages, Forest and conservation Experiment Station, School of Forestry, University of Montana, miscellaneous Paper No. 3.
- Stoekeler, E. G. (1959), "Airphoto Analysis of Terrain for Highway Location Studies in Maine," Photogrammetric Engineering, Vol. 25, No. 1, pp. 85-97.
- Suits, G. H. (1960), "The Nature of Infrared Radiation and Ways to Photograph It," Photogrammetric Engineering, Vol. 26, No. 5.
- Tanner, C. B. (1960), "Energy Balance Approach to Evapotranspiration from Crops," Soil Science, Society of American Proceedings, January-February.
- \_\_\_\_\_ (1963), "Plant Temperature," Agronomy Journal, VSS., pp. 210-211.
- Udall, S. L. (1965), "Resource Understanding - A Challenge to Aerial Methods," Photogrammetric Engineering, Vol. 31, No. 1, pp. 63-75.

VII. APPENDIX

## A. FILTER SPECTRAL ANALYSIS

During daytime operations it is necessary to filter out the short wavelength solar radiation energy since this energy is reflected rather than emitted by the surface. This was accomplished by using a silver sulphide polystyrene coated filter. Certain problems were encountered when making sky R-T measurements. It was noted that the radiometer was accepting radiation from a larger than 20 degree acceptance angle when measuring the sky R-T. The filter response was checked using a Beckman Infrared Spectrophotometer from 2 to 15 microns and a UV Beckman Spectrophotometer for the range from .4 to 2 microns. Tests confirmed that the filter is black to visible and near infrared radiation out to 3 microns. The spectral analysis curve is shown by Figure 17 for the portion of the spectrum from 2 to 15 microns.

The silver sulphide material is translucent to spectral energy beyond 3 microns. However, the polystyrene plastic coating has several absorption bands which result in transmission troughs across portions of the spectral analysis graph.

There is reason to suspect that the filter is undergoing heating when exposed directly to solar energy. The surface of the filter is not a perfect reflector; apparently it absorbs short wavelength energy. It is this absorption which results in heating of the filter and subsequent emission of long wavelengths heat energy through the filter increasing the apparent sky R-T measurement. The sky and sun R-T readings are still considered to be accurate relative measurements of the variation in atmospheric transparency.

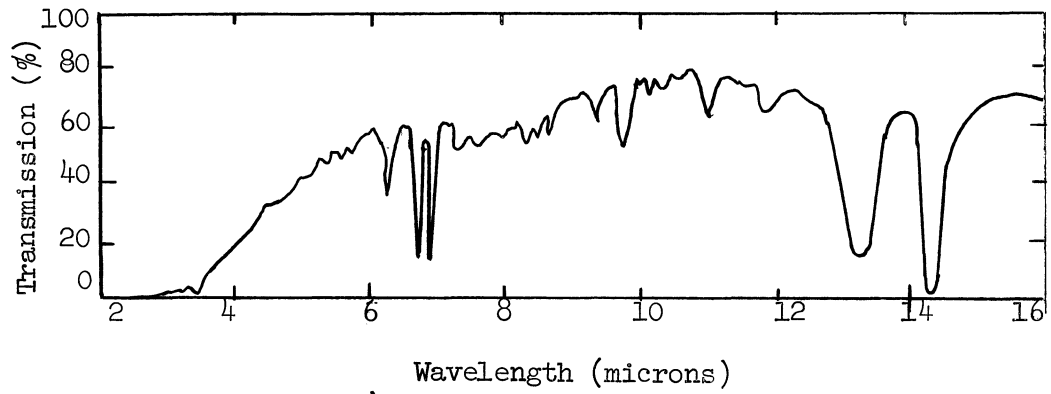


Figure 17. Spectral response curve for the silver sulphide, polystyrene coated filter used on the Stoll-Hardy radiometer.

## B. WEATHER SUMMARY

Meteorological conditions play an important part in determining surface R-T for given features. It is important in a study of this nature to maintain control over the weather conditions. A weather station was established in the Lindbergh Meadow (Figure 1) and continuous temperature and humidity records kept for the month of October. Other weather data were available from the Greenough Post Office and some were acquired from the Weather Bureau records at the Missoula County Airport.

Cloud type information was available only on days when data were collected at the Lindbergh Meadow. Precipitation recorded directly on the site would have been desirable; however, a rain gauge was located at the Greenough Post Office and the amount of precipitation was recorded on a weekly basis. Days of precipitation are estimated quite accurately by observing the relative humidity fluctuations as well as comparing days of precipitation at the Missoula County Airport with probable days of precipitation at the Greenough Post Office.

Average weather data for October, 1965 and for a nine-year average for October are given below (Steele, 1965):

	9 year avg.	1965
Average temperature for October	41.0°F	45.2°F
Minimum temperature for October	0.0°F	20.0°F
Maximum temperature for October	82.0°F	80.0°F
Average daily maximum temperature for October	55.2°F	62.7°F
Average daily minimum temperature for October	26.7°F	27.7°F
Average daily minimum relative humidity for Oct.	40.7%	35.7%
Precipitation for October	1.2"	0.17"

TABLE 11. GREENOUGH POST OFFICE WEATHER STATION DATA FOR OCTOBER, 1965

Date	Temp. (°F)		RH Min	Wind		Weekly Precip. <sup>3</sup>	Sky Cover	Insolation Received <sup>5</sup>
	Max.	Min.		Acum <sup>1</sup>	Mph <sup>2</sup>			
1	70	26	19	41	3.5	0	4	100%
2	72	28	26	57	5	0	6	100
3	76	30	26	45	4	0	3	97
4	70	32	24	46	4	0	9	57
5	57	32	46	39	3	0	10	16
6	64	32	38	76	6	0	6	68
7	68	38	40	120	10	0	3	90
8	80	32	22	114	10	0	7	79
9	72	31	30	74	6	0	3	100
10	68	32	29	88	7	0	1	89
11		26	34	67	6	0	0	86
12	64	26	28	45	4	0	8	31
13	54	30	54	39	3	T	10	18
14	59	30	44	40	3	0.06	9	35
15	46	36	50	56	5	0.06	10	4
16	50	20	32	54	5	0	0	96
17	50	26	40	41	4	T	10	7
18	58	30	43	41	4	T	9	18
19	48	24	56	51	4	0.05	9	27
20	58	22	36	60	5	0	9	52
21	62	25	38	59	5	0	9	55
22	59	25	44	53	4	0	9	83
23	66	24	34	36	3	0	3	77
24	73	26	28	67	5	0	7	60
25		26		43	4	0	1	84
26				50	4	0	1	85

1. Accumulative daily wind in Mph.
2. Accumulative divided by 12.
3. Precipitation occurrence for a particular day based on R. H. and Temperature trends.
4. From Missoula County Airport tenths of sky covered by clouds.
5. Percent of insolation reaching earth's surface out of total possible recorded at the weather bureau, Missoula County Airport.

TABLE 12. LINDBERGH MEADOW WEATHER FOR OCTOBER, 1965

Date	Temperature		Relative Humidity		Cloud Cover
	Min (°C)	Max (°C)	Min	Max	
2	-2	24	24	100	
3	-2	23	24	100	
4	-2	21	28	100	
5	1	13	48	100	
6	2	18	38	100	
7	7	18	42	94	
8	0	24	20	100	
9	2	20	32	100	scattered cirrus
10	0	18	28	100	
11	-1	18	32	100	
12	-3	16	28	88	thin altostratus
13	3	12	46	100	
14	-2	15	38	100	
15	-1	8	44	92	
16	-3	8	28	92	clear all day
17	-3	9	34	96	
18	-1	13	37	100	
19	-2	9	48	100	
20	-4	14	32	100	
21	-4	15	30	100	
22	-4	17	34	100	
23	-5	19	28	100	clear with some
24	-4	19	22	98	smoke in pm
25	-3	20	22	100	
26	-4	18	26	100	very high thin cirrus

TABLE 13. HOURLY WEATHER DATA FOR SAMPLE DAYS DURING OCTOBER, 1965

Time	Air temperature (°C)					Relative humidity (%)					Wind (mph)				
	Dates					Dates					Dates				
	9	12	16	23	26	9	12	16	23	26	9	12	16	23	26
800	10	-3	-2	-4	-2	70	96	82	98	94	0	0		0	
900	12	2	2	2	3	58	86	60	82	76		0			
1000	16	6	4	5	7	43	70	52	70	58	0	1-2			0
1100	18	9	5	8	10	43	56	47	58	46	3-4	1-2	5-6	1-2	
1200	19	15	6	11	12	35	38	38	46	38		5-6	5-6	0	0
1300	20	16	7	14	15	33	35	34	36	32	7-8	5-6	5-6	0	1-2
1400	20	16	8	17	17	32	30	30	30	27		3-4			
1500	20	16	8	18	18	31	32	30	32	27		1-2	5-6	0	1-2
1600	19	15	8	18	18	32	36	32	28	32	5-6	0	5-6	0	
1700	19	14	7	13	10	32	54	34	52	64					0
1800	13	10	5	7	4	42	72	40	84	83	0	0	1-2	0	
1900	7	7	2	4	2	78	82	60	92	90	0	0		0	0
2000	5	5	1	2	0	86	89	62	97	95		0	0		0
2100	4	4	0	1	0	96	90	74	98	98		0		0	
2200	3	4	-2	0	-1	100	89	84	100			0		0	
2300	2	4	-2	-1	-1	90	86	90	90		0			0	
2400	2	4	-3	-1	-2	92	90	82	80			0		0	
*0100	1	4	-2	-2	-3	92	90	82	80		0				
0200	1	6	0	-2	-3	82	80	70	80						
0300	1	7	0	-3	-3	70	80	69	84	98					
0400	0	7	0	-3	-4	69	84	98	100						
0500	0	7	-1	-3	-4	74	88	96	99						
0600	0	7	-2	-3	-5	70	94	96	98						
0700	-1	7	-2	-3	-5	100	70	94	95	96	0		0		

\*continuing into the next day with the weather data.



TABLE 14. HOURLY WEATHER DATA FOR SAMPLE DAYS DURING OCTOBER, 1965.

Time	Sky temperature (°C)					Sun temperature (°C)					Cloud cover <sup>1</sup>				
	Dates					Dates					Dates				
	9	12	16	23	26	9	12	16	23	26	9	12	16	23	26
0800		-4.9		-7.1			18.7		24.5		02	02		01	
0900			-10.6					7.5					08		
1000	12.5	4.5			0.3	31.8	27.3			27.1	01	02			01
1100	14.4	9.6	0.9	2.5		31.9	29.5	28.0	27.6		01	01	01	01	
1200		9.7	-0.1	7.0	4.4		29.0	27.6	29.3	28.5		01	01	01	02
1300	15.3	11.3	-1.1	9.2	8.6	31.9	28.0	27.9	30.6	30.1	01	05	01	01	02
1400		7.5						16.3				06			
1500		8.0	-4.7	5.4	5.5		11.9	27.3	31.4	30.7		04	01	01	02
1600	7.1	4.9	-12.2	1.8		25.0	4.8	24.6	29.1		03	04	01	01	
1700					-18.4										01
1800	-11.7	-7.4	-30.0	-18.6							01	04	01	01	
1900	-14.6	-9.1		-19.3	-20.3						01	06		01	01
2000			-28.5		-21.7								01		01
2100		-2.9		-22.4								06		01	
2200			-27.6										01		
2300	-13.9			-22.5							01			01	
2400			-5.3	-23.0									04	01	
0100 <sup>2</sup>															
0200	-12.8										04				
0300															
0700	-12.3		-0.4								01		10		

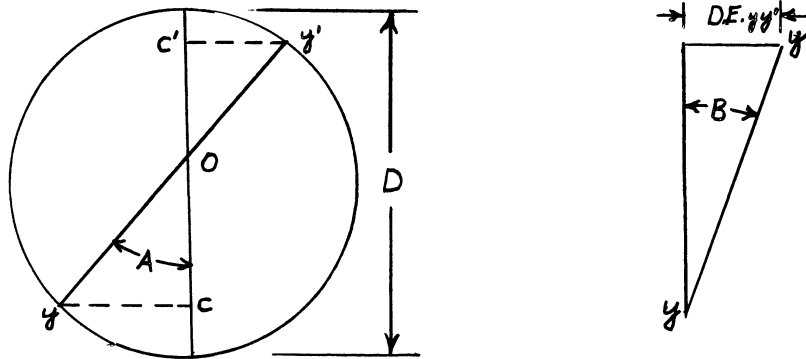
<sup>1</sup> 01 Clear; 02 scattered thin cirrus; 03 continuous cirrus cover; 04 Cloudy; 05 High partial overcast; 06 High cloud cover; 07 Sun broke through clouds; 08 Hazy; 10 Thin altostratus layer.

<sup>2</sup> Continuing into the next day with the weather data.

C. METHOD FOR DETERMINING INSOLATION ANGLE OF  
INCIDENCE GIVEN THE ASPECT AND SLOPE

It was necessary to accurately describe the relative angles of insolation incidence for a given combination of aspect, slope, and time for each sample point. The sun's bearing and elevation were calculated for five time periods and graphed as shown by Figure 19. From this graph, the sun's inclination and elevation can be read for any time period between 1000 and 1500 hours for October 23, 1965. The trigonometric considerations in determining the insolation angle of incidence for a given plot point and for a specific time are outlined below:

Figure 18.



- A = the horizontal angle from the aspect direction to the sun.
- B = the vertical angle from a horizontal plane to the sample plot plane.
- D = the sample point diameter which is about 20 inches.
- D.E. = the difference in elevation in inches from the horizontal plane along  $\overline{yy'}$

Equation 1.  $CC' = 2\overline{OO} = D(\cos A)$

Equation 2.  $\frac{D.E. yy'}{h} = \frac{CC'}{D}$

Equation 3.  $\sin B = \frac{D.E. yy'}{D}$

Substituting equation 1. into equation 2.

$$\text{Equation 4.} \quad D \cdot E \cdot \cos A = \frac{D(\cos A) h}{D}$$

Substituting equation 3. into equation 4.

$$\text{Equation 5.} \quad D(\sin B) = (\cos A) h$$

$$\text{or,} \quad \sin B = \frac{(\cos A) h}{D}$$

$$\text{so,} \quad \sin B = \frac{(\cos A) h}{20''} = .05 (\cos A) h$$

The equation,  $\sin B = .05 (\cos A) h$ , describes the functional relationship between the sun's bearing from the direction of aspect represented by "A" and the amount of slope in inches from one side of the plot to the other along the direction of aspect being represented by "h". The amount of slope was determined by placing a carpenter's level across the plot in the direction of aspect and measuring the distance to the plot plane from the horizontal level plane. The above equation is represented graphically for various slope and bearing combinations and gives the deviation in angle of incidence from the horizontal plane (Figure 20). The corrected angles of insolation incidence by time and sample point are listed in Table 15. Sites VII and III did not have significant differences in aspect and slope between sample points.

The procedure employed for finding the angles of insolation incidence for each sample point is similar to that for the example illustrated below:

## FIELD DATA MEASUREMENTS:

Site II; sample plot 6; south aspect; 3 inch slope  
23 October, 1965; time, 1130.

## REFERRING TO FIGURE 19:

Sun's elevation =  $30.5^{\circ}$ .  
Sun's bearing =  $S12^{\circ}E$ .

## REFERRING TO FIGURE 20:

Azimuth =  $12^{\circ}$ .  
Slope = 3 inches.  
Deviation in angle of insolation incidence as a result  
of the sample plot slope equals  $8.4^{\circ}$ .

ANGLE OF INSOLATION INCIDENCE FOR THE ABOVE TIME AND CONDITIONS  
 $30.5^{\circ}$  plus  $8.4^{\circ}$  =  $38.9^{\circ}$ .

The angles of insolation incidence thus computed (Table 15) are angles in the vertical plane between the sun's ray and the intersection line between the vertical plane and the sample plot plane. A more rigorous treatment of the problem requires the angle of insolation incidence to be measured in the plane which is perpendicular to the plot plane and contains a sun's ray. Since the sample plot planes had small slopes, the differences between these two methods for calculating angles of insolation incidence were found to be negligible.

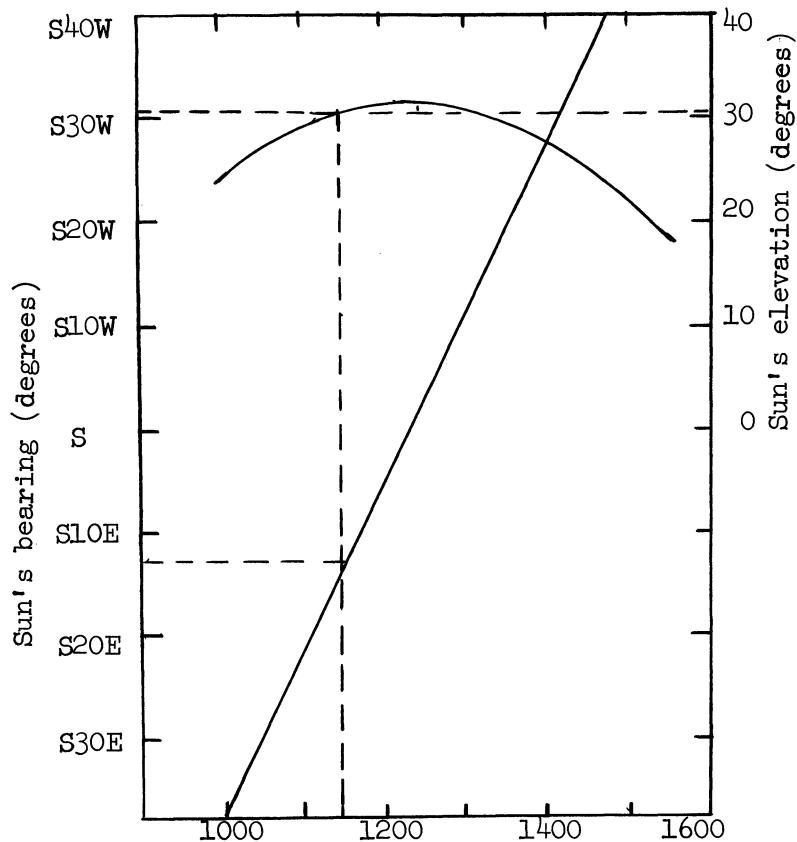


Figure 19. Bearing and elevation of sun as a function of time.

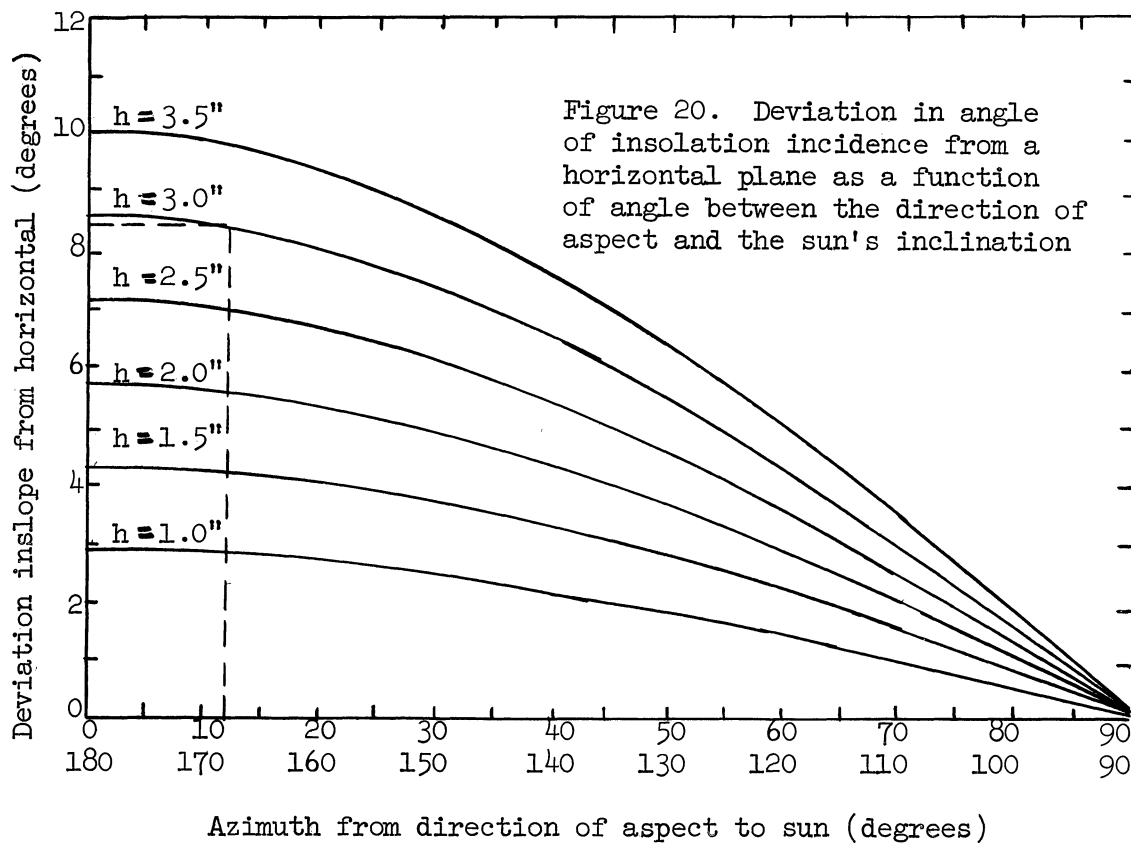


Figure 20. Deviation in angle of insolation incidence from a horizontal plane as a function of angle between the direction of aspect and the sun's inclination

TABLE 15. ANGLE OF INSOLATION RECEIPT FROM PLOT PLANE (OCTOBER 1965)

Sample Point	Aspect	Slope	Angles of incidence (Degrees)				
			TIME				
			1030	1130	1230	1330	1430
<u>SITE I</u>							
1	N	1"	24.5	27.7	29.1	27.3	22.1
2	NW	3"	18.7	23.1	26.4	26.4	23.0
3	NW	1"	24.2	28.0	30.1	28.8	24.0
4	NW	2"	21.5	25.6	28.1	27.6	23.5
5	SW	1"	27.7	32.0	34.2	32.6	27.3
6		Level	27.0	30.5	32.0	30.0	24.5
7	N	1"	24.5	27.7	29.1	27.3	22.1
8		Level	27.0	30.5	32.0	30.0	24.5
9	SW	2"	28.5	33.4	36.3	35.2	30.1
10	NW	3"	18.7	23.1	26.4	26.4	23.0
11	NW	1"	24.5	27.7	29.1	27.3	22.1
12	NW	1"	24.5	27.7	29.1	27.3	22.1
<u>SITE II</u>							
1		Level	27.0	30.5	32.0	30.0	24.5
2	S	1"	29.5	33.3	34.9	31.7	26.9
3	W	1"	25.6	29.8	32.2	31.0	26.2
4	N	2"	22.0	25.0	26.3	24.6	19.8
5	N	2"	22.0	25.0	26.3	24.6	19.8
6	S	3"	34.5	38.9	40.6	38.1	31.6
7	NW	1"	24.2	28.0	30.1	28.8	24.0
8	W	1"	25.6	29.8	32.2	31.0	26.2
9	W	1"	25.6	29.8	32.2	31.0	26.2
10	NW	1"	24.2	28.0	30.1	28.8	24.0
11	SW	2"	28.5	33.4	36.3	35.2	30.1
12	N	1"	24.5	27.7	29.1	27.3	22.1
<u>SITE IV</u>							
1	N	1"	24.5	27.7	29.1	27.3	22.1
2	N	1"	24.5	27.7	29.1	27.3	22.1
3	S	3"	34.5	38.9	40.6	38.1	31.6
4	NW	3"	18.7	23.1	26.4	26.4	23.0
5	W	1"	25.6	29.8	32.2	31.0	26.2
6	S	2"	32.0	36.1	37.7	35.4	29.2
7	NE	1"	26.3	29.0	29.8	27.4	21.7
8	N	1"	24.5	27.7	29.1	27.3	22.1
9		Level	27.0	30.5	32.0	30.0	24.5
10	N	1"	24.5	27.7	29.1	27.3	22.1
11	NW	1"	24.2	28.0	30.1	28.8	24.0
12	W	1"	25.6	29.8	32.2	31.0	26.2

TABLE 15 (Continued)

Sample Point	Aspect	Slope	Angles of incidence (Degrees)				
			TIME				
			1030	1130	1230	1330	1430
<u>SITE V</u>							
1	N	1"	24.5	27.7	29.1	27.3	22.1
2		Level	27.0	30.5	32.0	30.0	24.5
3	E	Level	27.0	30.5	32.0	30.0	24.5
4							
5	E	1"	28.5	31.2	31.8	29.0	23.3
6		Level	27.0	30.5	32.0	30.0	24.5
7	NW	1"	24.2	28.0	30.1	28.8	24.0
8		Level	27.0	30.5	32.0	30.0	24.5
9	N	1"	24.5	27.7	29.1	27.3	22.1
10		Level	27.0	30.5	32.0	30.0	24.5
11	Level	1"	24.5	27.7	29.1	27.3	22.1
12		Level	27.0	30.5	32.0	30.0	24.5
<u>SITE VI</u>							
1	W	1"	25.6	29.8	32.2	31.0	26.2
2		Level	27.0	30.5	32.0	30.0	24.5
3	NW	Level	27.0	30.5	32.0	30.0	24.5
4		1"	24.2	28.0	30.1	28.8	24.0
5	NW	Level	27.0	30.5	32.0	30.0	24.5
6		Level	27.0	30.5	32.0	30.0	24.5
7	W	1"	24.2	28.0	30.1	28.8	24.0
8		Level	27.0	30.5	32.0	30.0	24.5
9	SW	1"	25.6	29.8	32.2	31.0	26.2
10		Level	27.0	30.5	32.0	30.0	24.5
11	NW	1"	27.7	32.0	34.2	32.6	27.3
12		Level	24.2	28.0	30.1	28.8	24.0

D. PHOTOGRAPHS OF SELECTED FEATURES



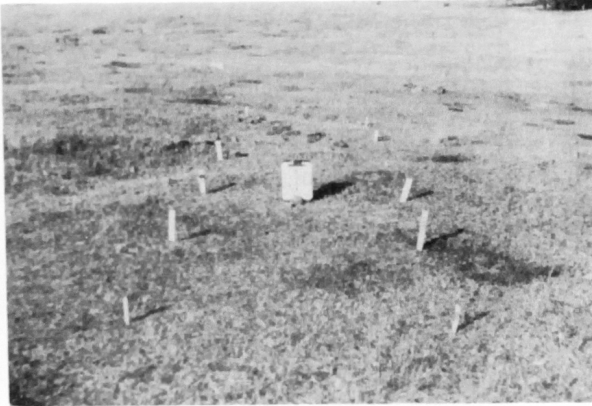


Figure 21. Photograph of Site I. This site is moderately well drained and was one of the driest sites.



Figure 22. Photograph of Site II. This site is intermediate in moisture content and is not as well drained as site I.



Figure 23. Photograph of Site III. This site is poorly drained and has evidence of surface seepage present.



Figure 24. Photograph of site IV. This site compares to site I in vegetation, soil and soil moisture.



Figure 25. Photograph of site V. This site is much like site II. It is poorly drained and intermediate in moisture content.



Figure 26. Photograph of site VI. This site is very similar to site V and is intermediate in soil moisture.

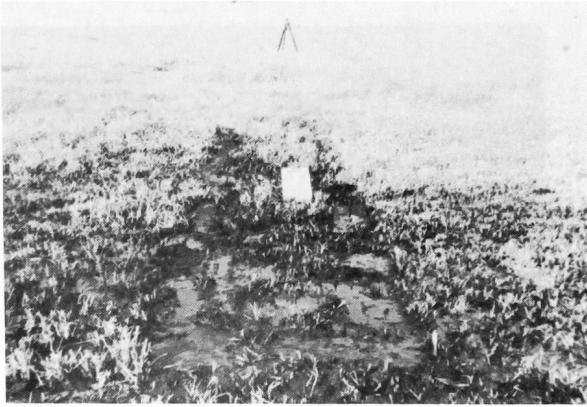


Figure 27 Photograph of site VII. This site is very poorly drained and it has 2-3 inches of standing to moving water. It is a sedge peaty swamp.



Figure 28. Photograph of reservoir edge; water is from 6-12 inches deep along the sample line between the stakes.



Figure 29. Photograph of the large quartzite rock showing the south exposure which was sampled during the study.

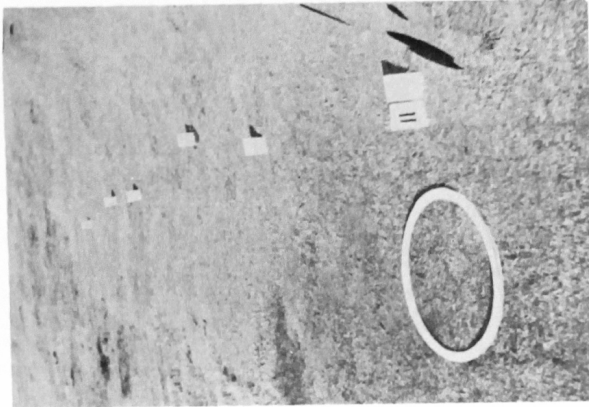


Figure 32. Photograph of the clipped paired plot for site II.

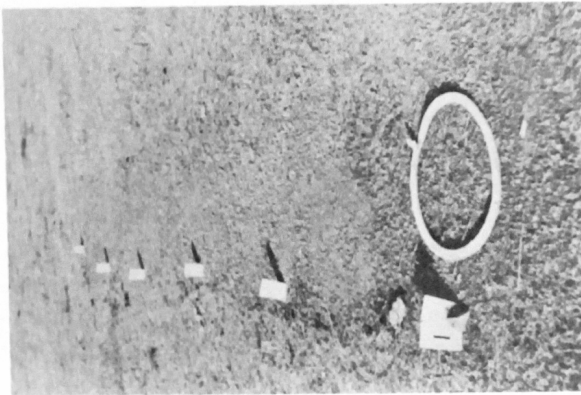


Figure 31. Photograph of the clipped paired plot for site I.

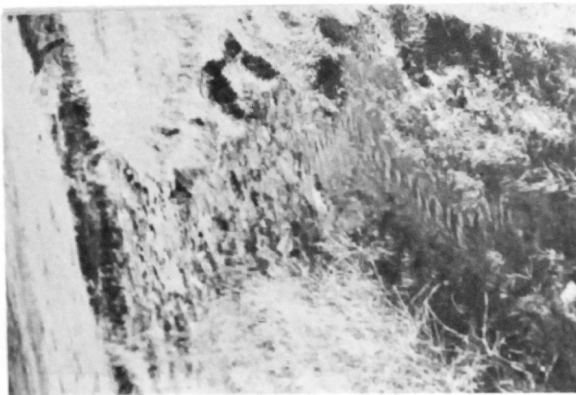


Figure 30. Photograph of stream just before it discharges into reservoir. This is the general portion of the stream which was sampled using the radio-meter.

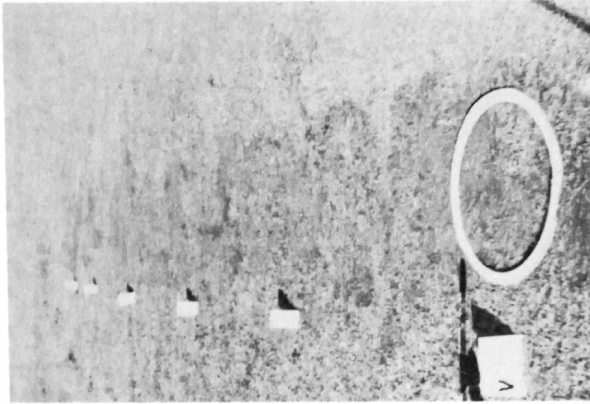


Figure 35. Photograph of the clipped paired plot for site V. Sites II, V and VI appear to be quite similar in surface characteristics.

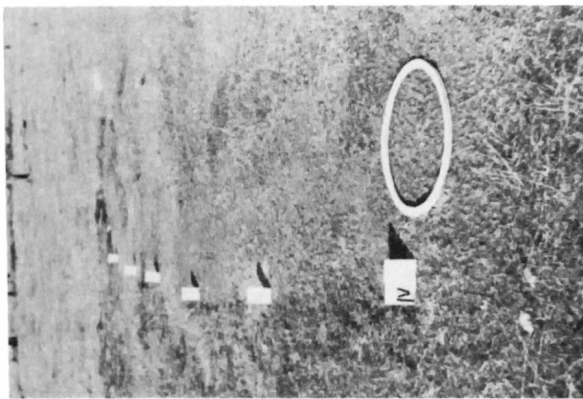
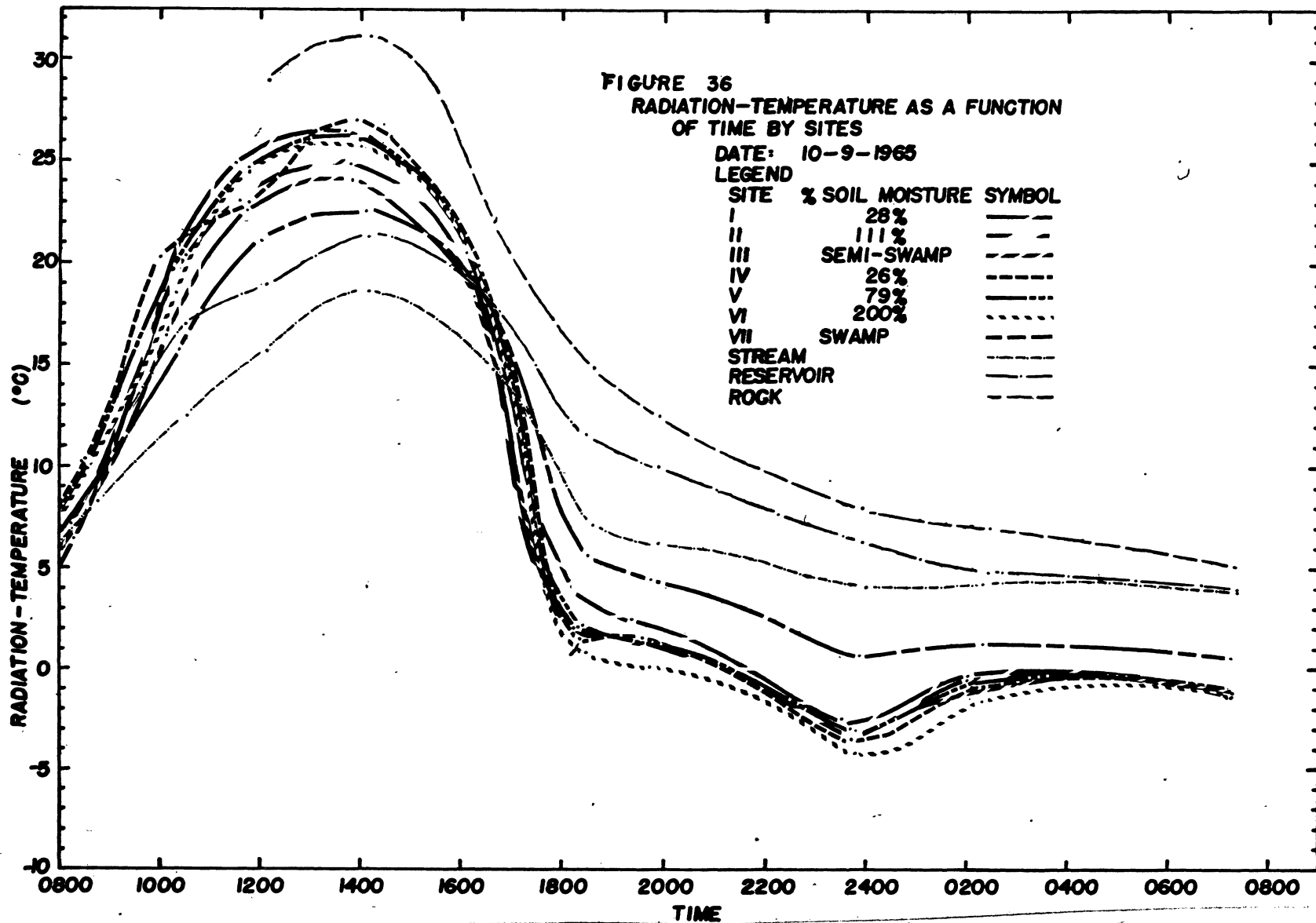


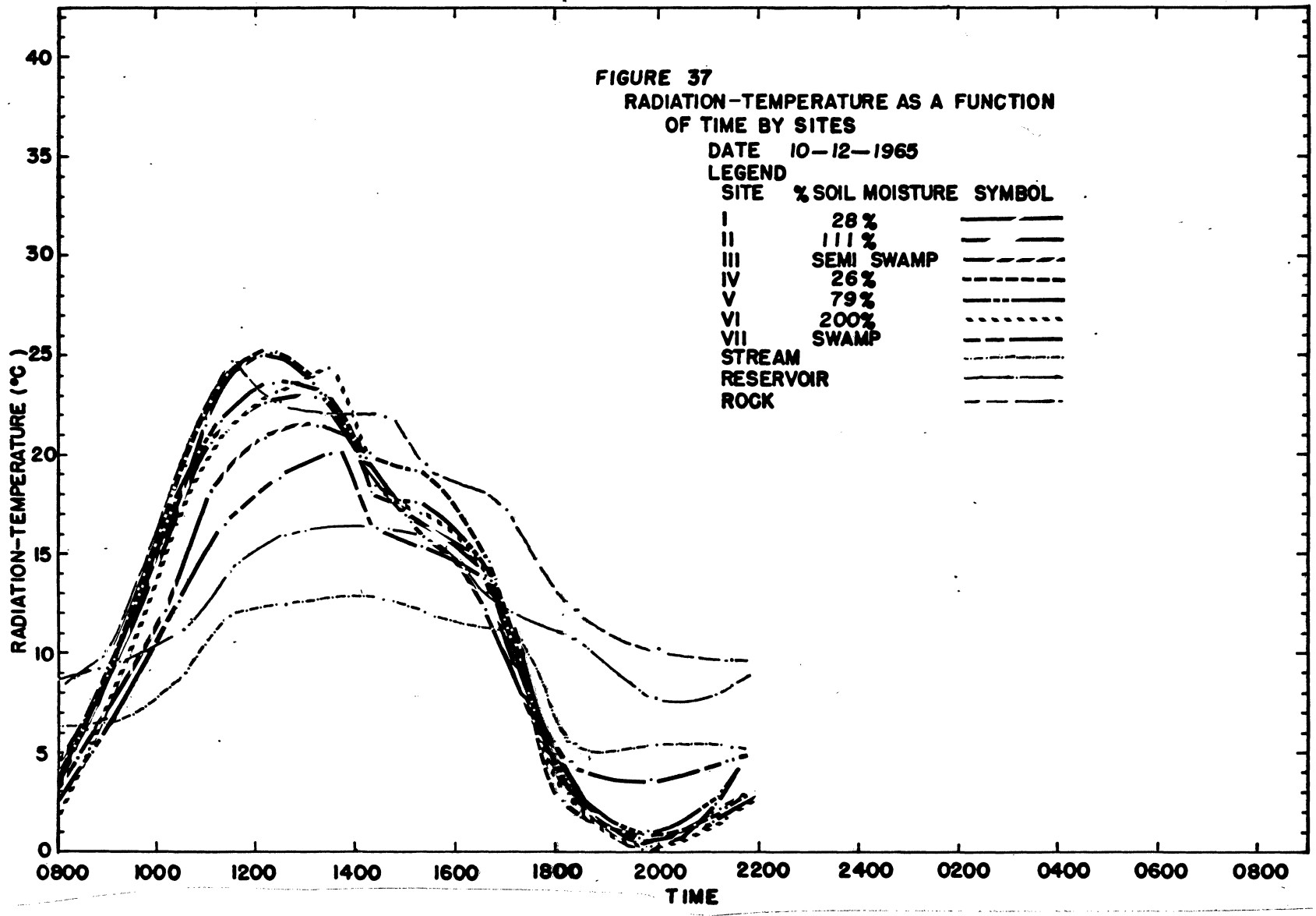
Figure 34. Photograph of clipped paired plot for site IV. This is quite similar to site I.



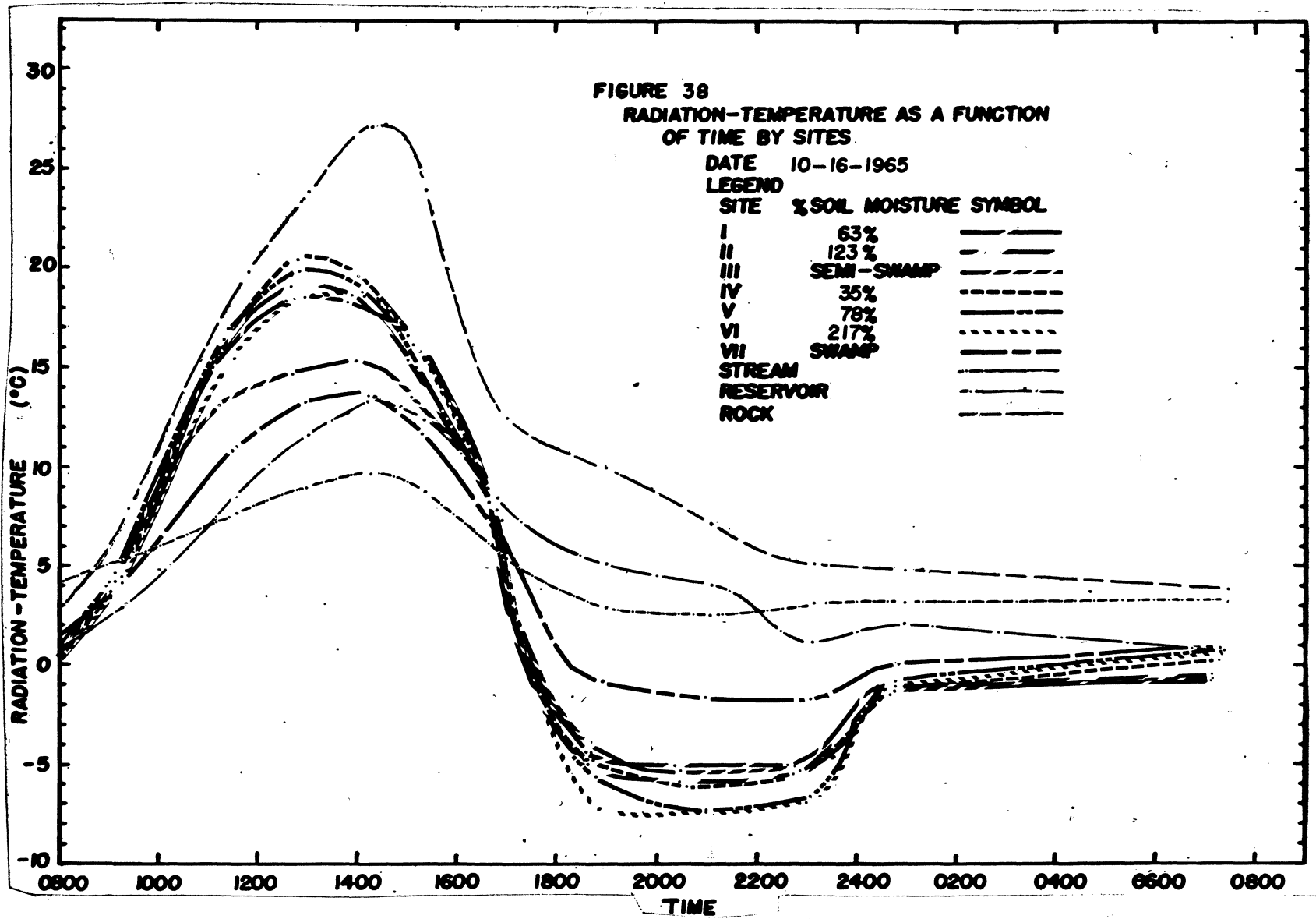
Figure 33. Photograph of the clipped paired plot for site III. Due to the surface moisture this plot was clipped low exposing the dark organic horizon.

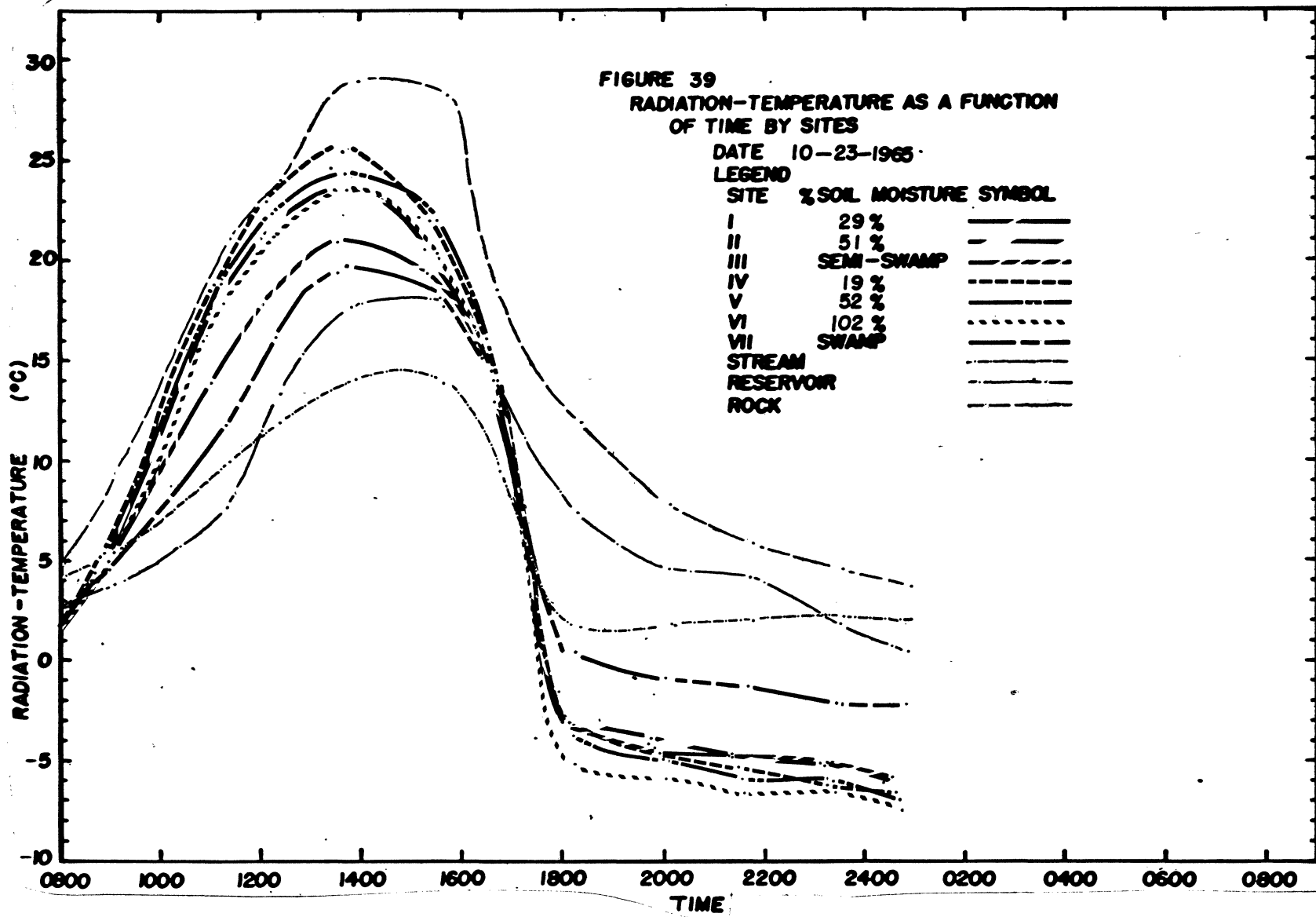
E. GRAPHS OF MEAN RADIATION-TEMPERATURE VALUES

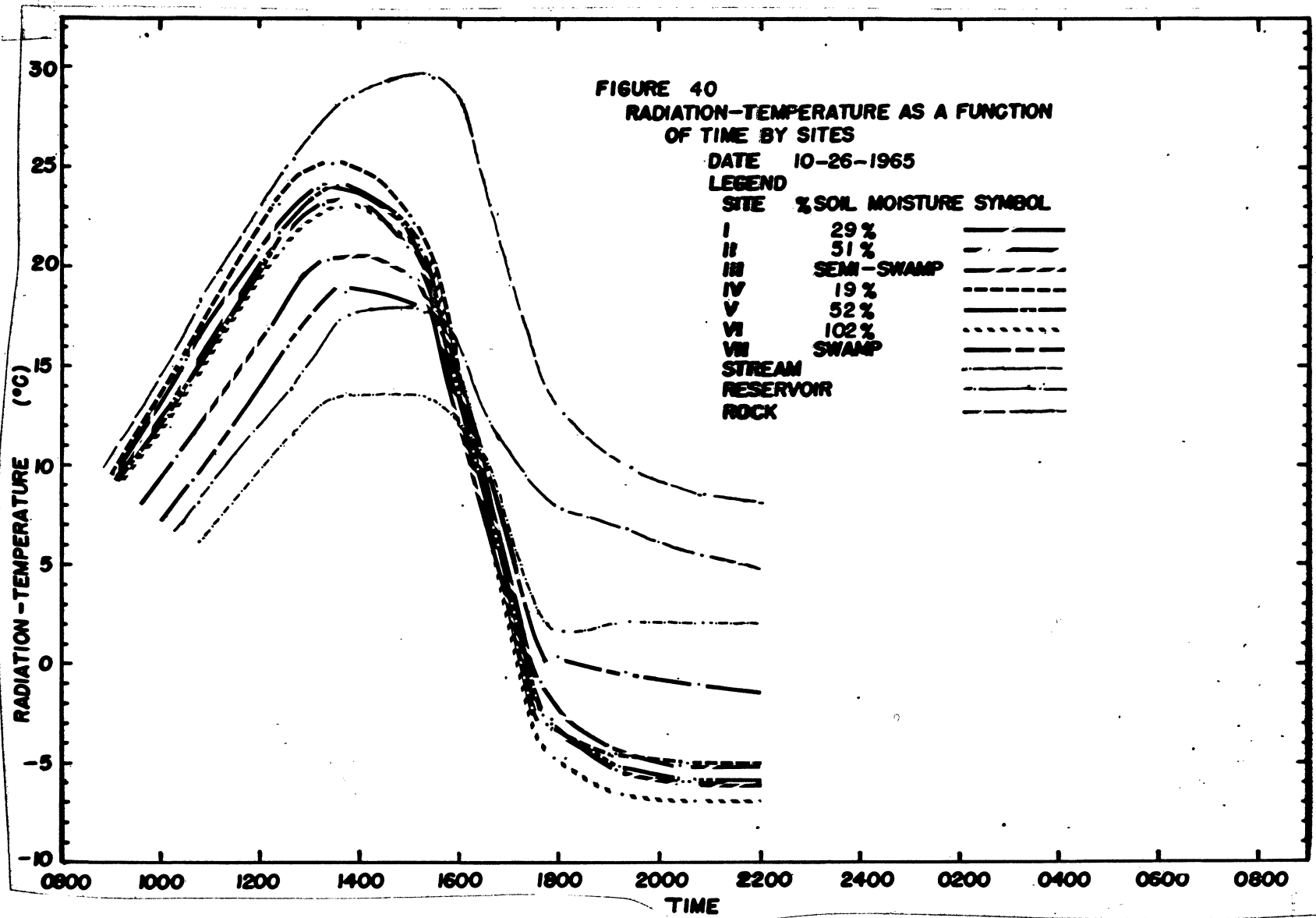












## F. ADJUSTMENT OF R-T MEANS

The R-T data was collected over a twenty minute time period in most cases. It would be desirable to acquire all R-T readings simultaneously for a given sample period. But this was not practical or possible with the instrumentation available. An alternative is to adjust the R-T site means to one point in time for a given sample period.

To do this accurately, expanded scales were used in graphing the mean R-T values for the seven sites during the peak radiation emission periods (Figures 42 to 46). Figure 41 illustrates the mechanics involved in adjusting the means. The symbols  $\odot$ ,  $\triangle$ , and  $\square$  represent sites I, II and III respectively. The vertical line projected through the sample period indicates the time we wish to adjust all our means around. Thus, if  $\Delta y_I$  is added to each R-T value for site I, the mean of these corrected values will fall on the intersection of the vertical line and the curve drawn through the means for site I. The value  $\Delta y_{II}$  would be subtracted from each value for site II and no addition or subtraction would be necessary for site III.

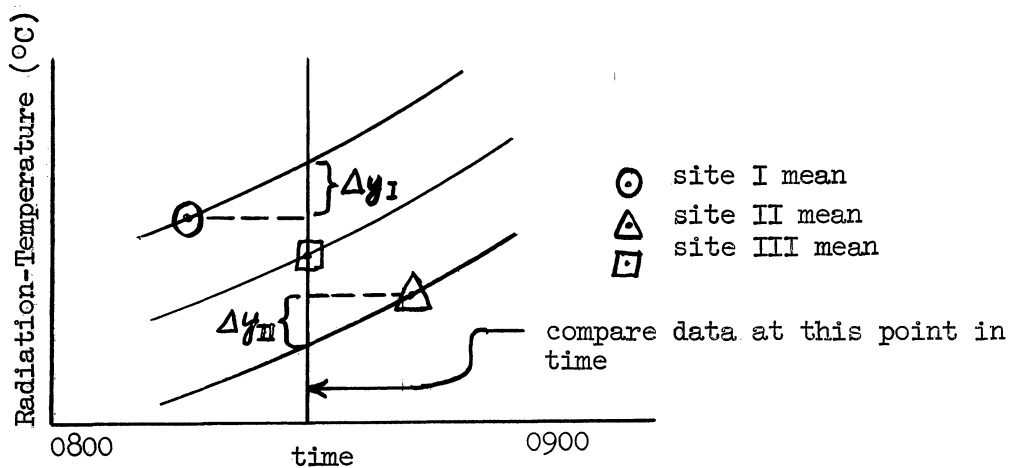
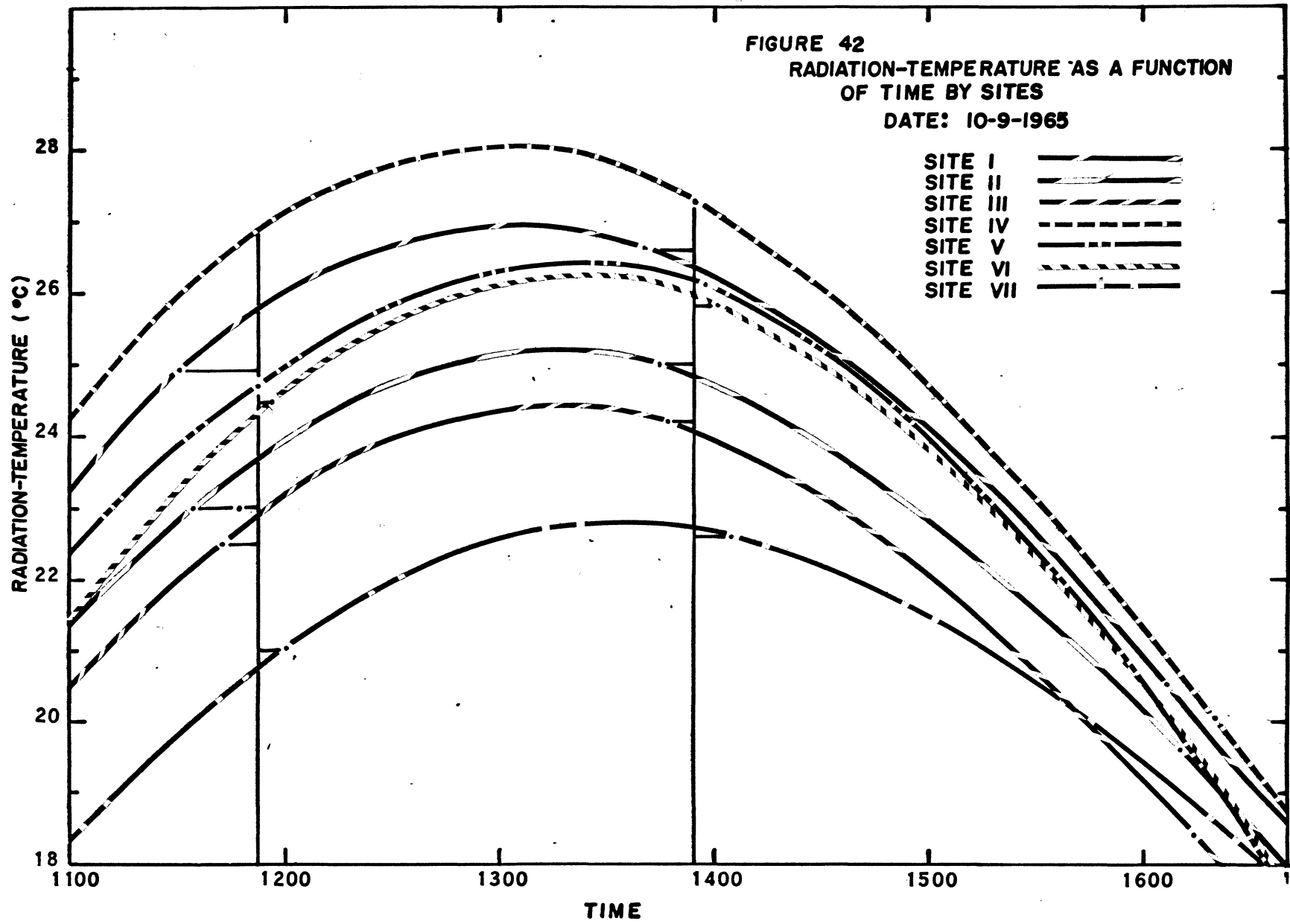


Figure 41. Adjustment of R-T to one point in time.

G. GRAPHS OF MEAN RADIATION-TEMPERATURE VALUES  
FOR THE PEAK INSOLATION RECEIPT PERIODS

FIGURE 42  
RADIATION-TEMPERATURE AS A FUNCTION  
OF TIME BY SITES  
DATE: 10-9-1965



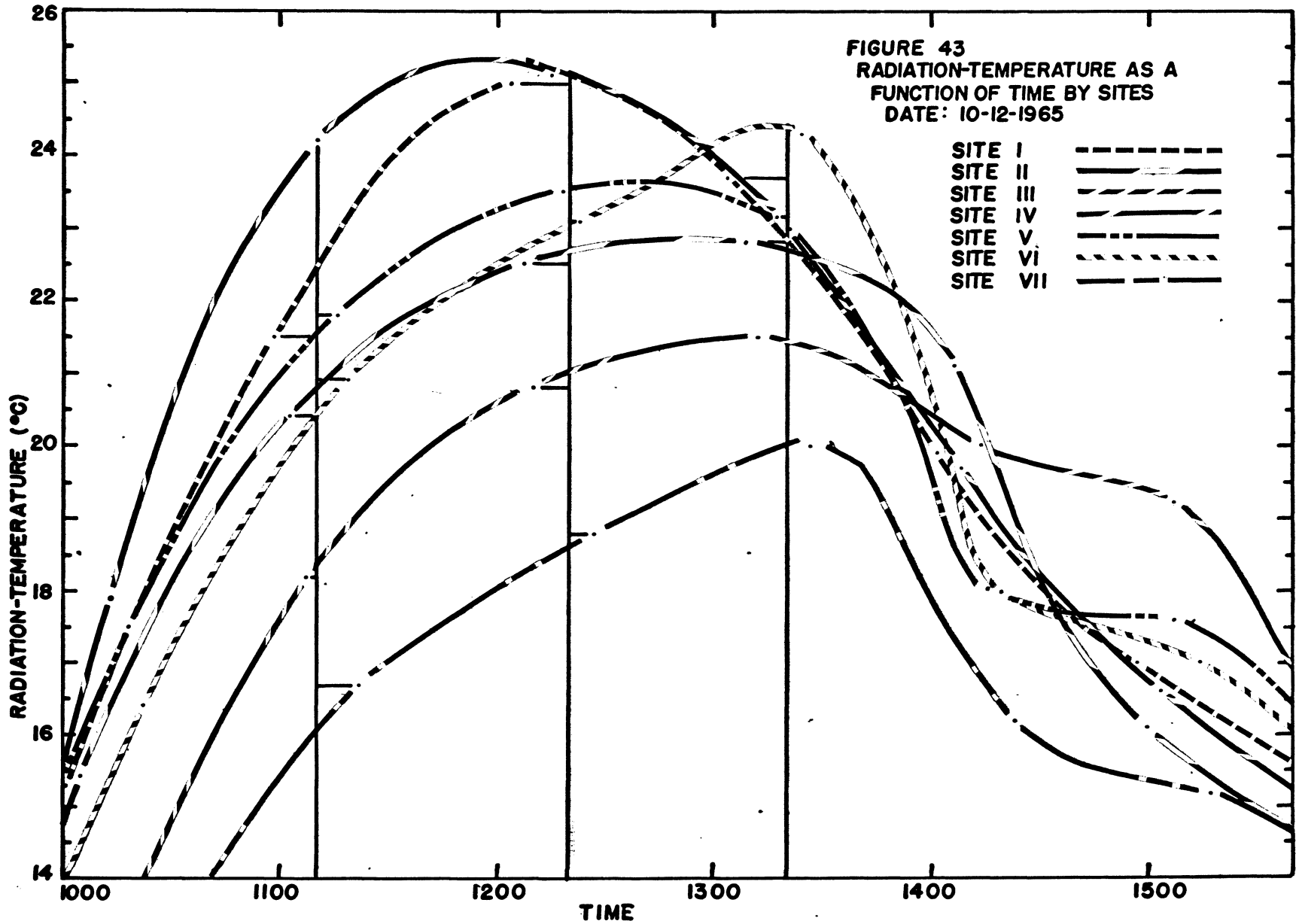
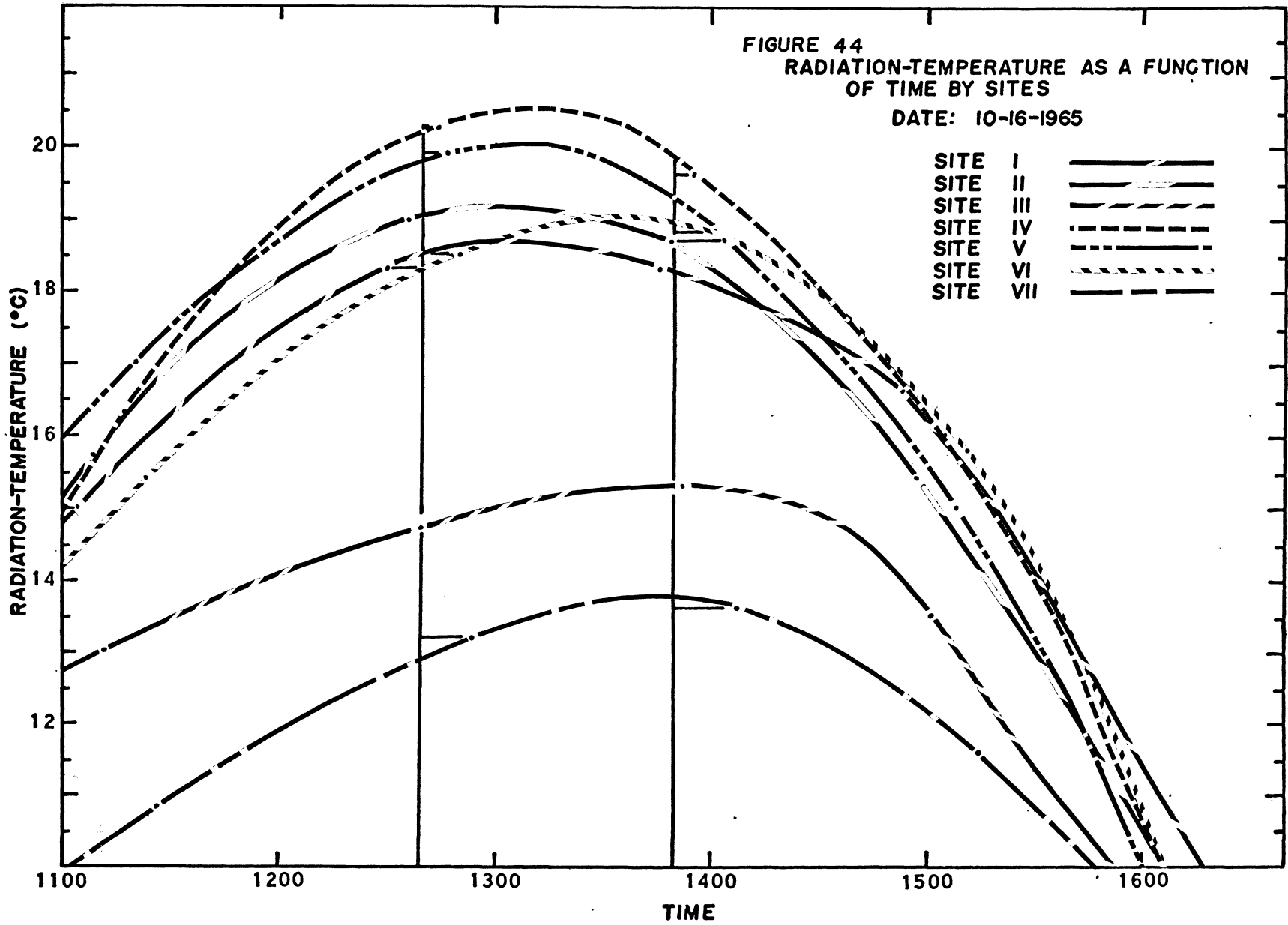
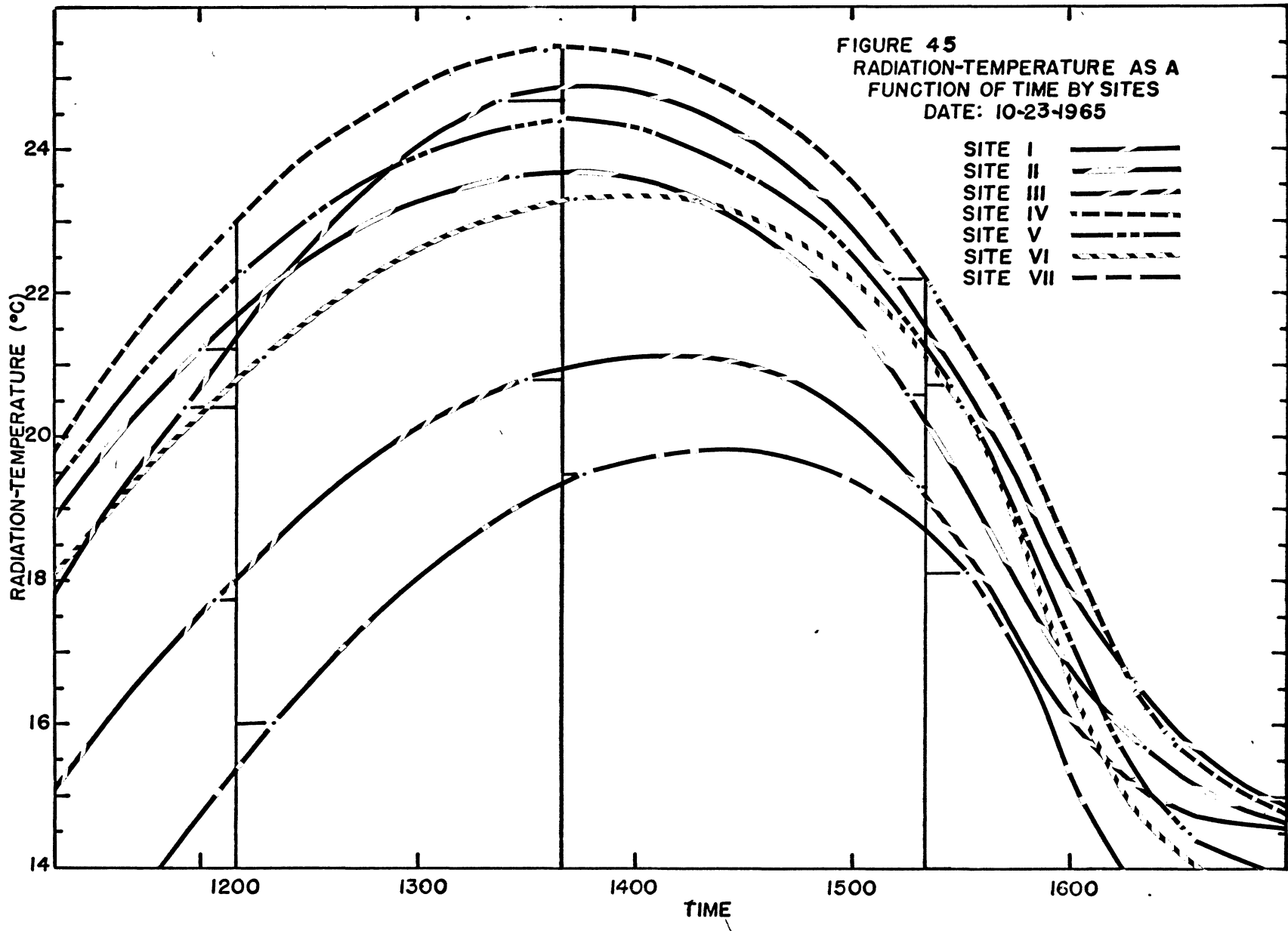


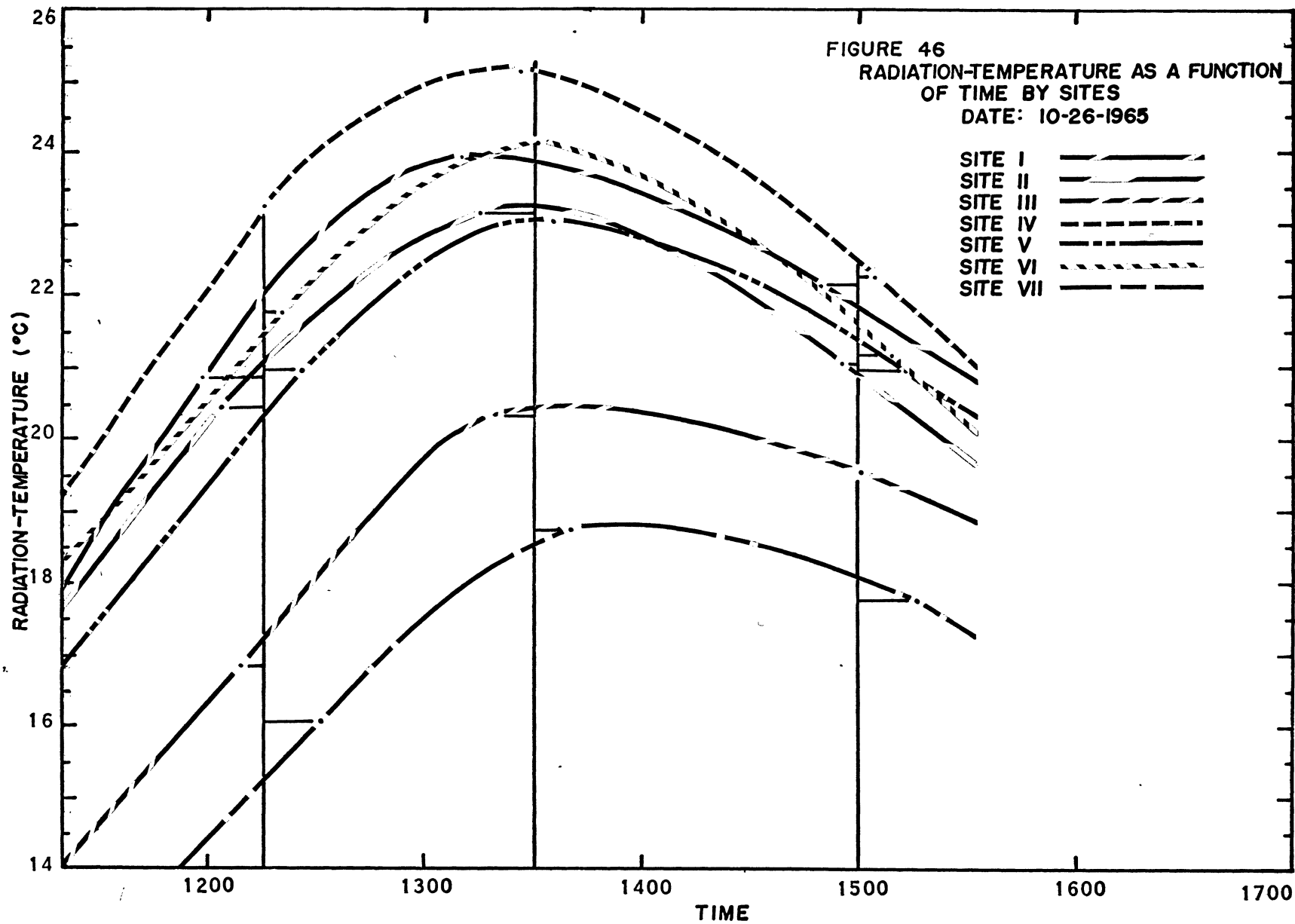
FIGURE 44  
RADIATION-TEMPERATURE AS A FUNCTION  
OF TIME BY SITES

DATE: 10-16-1965

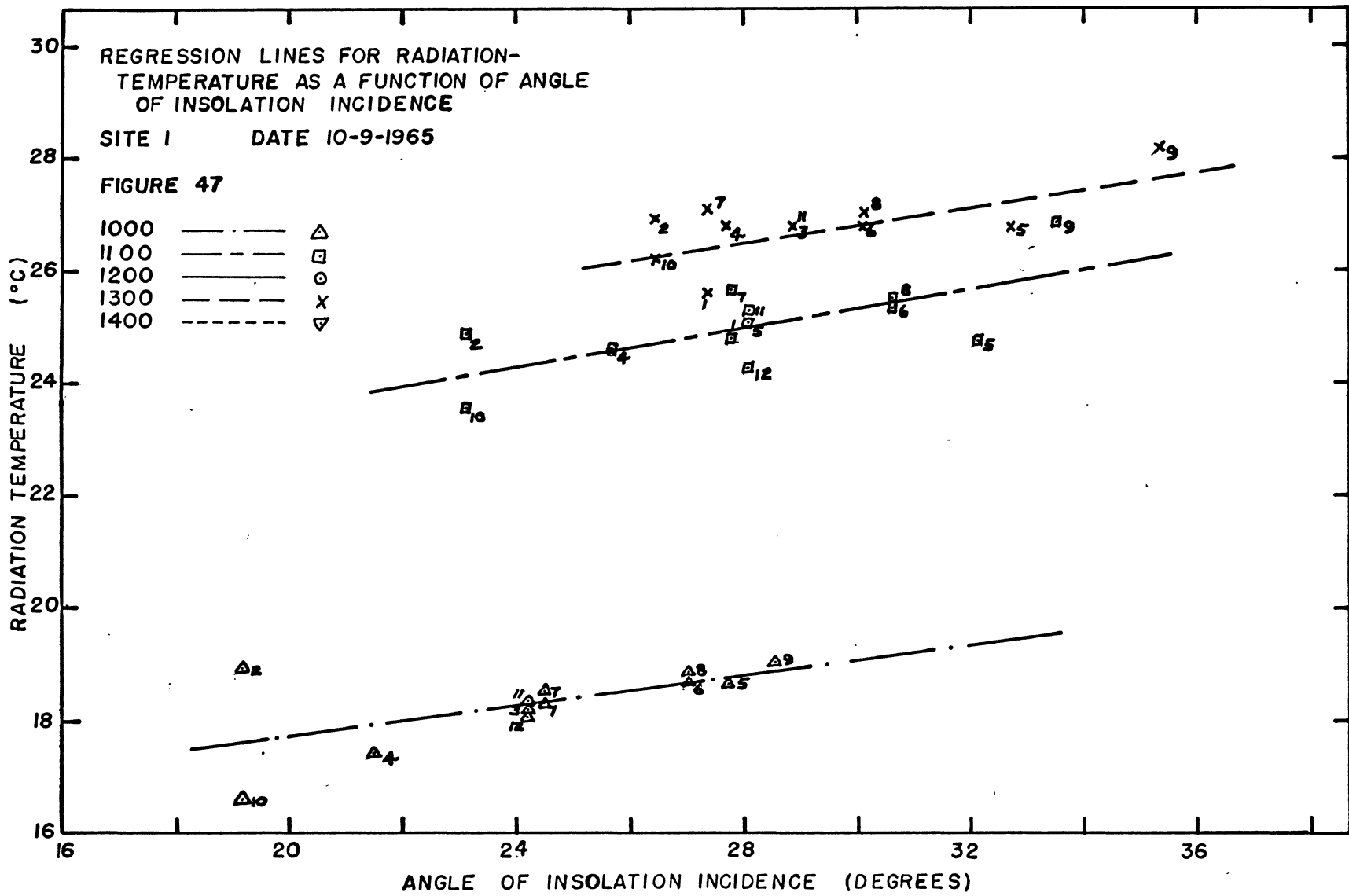


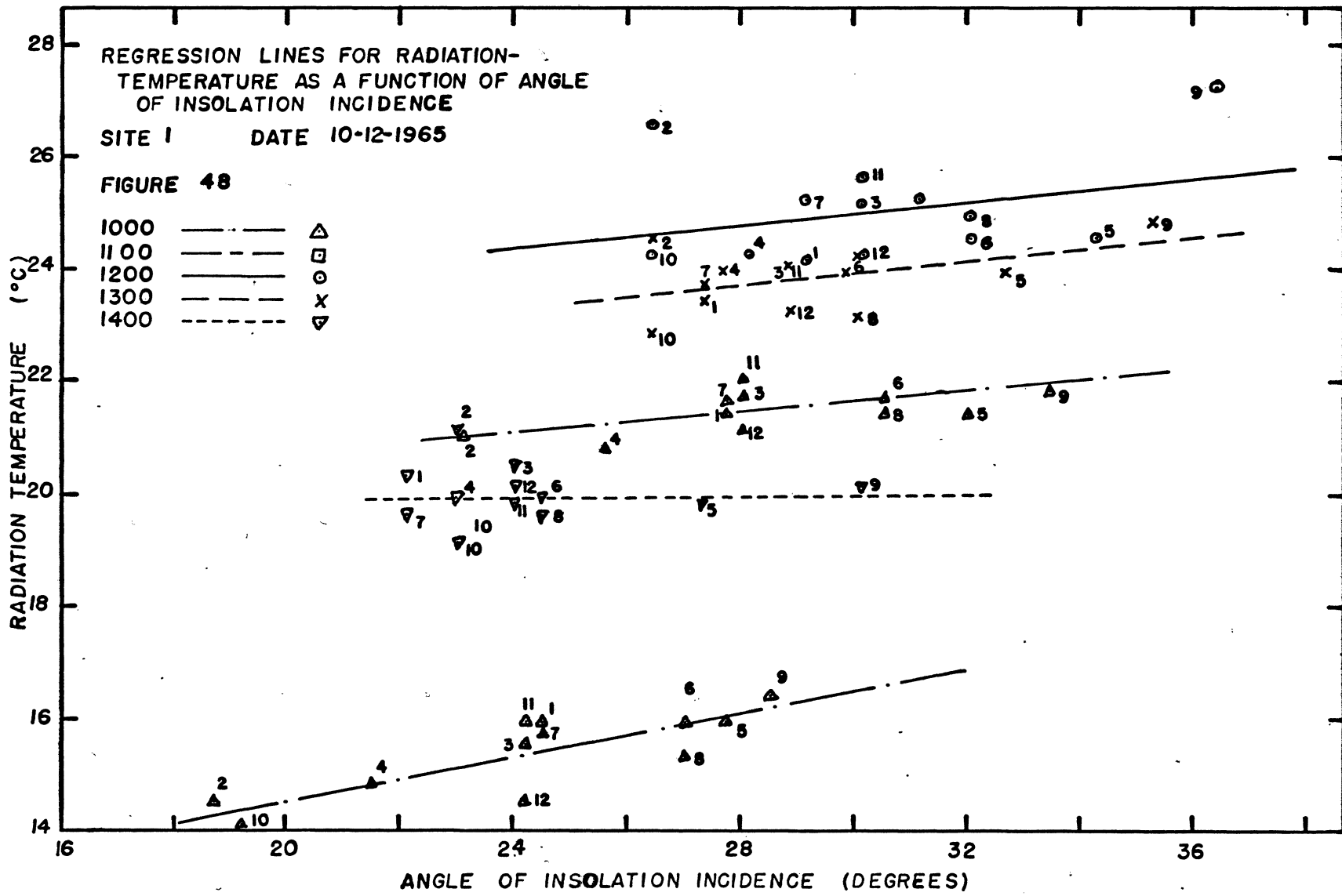


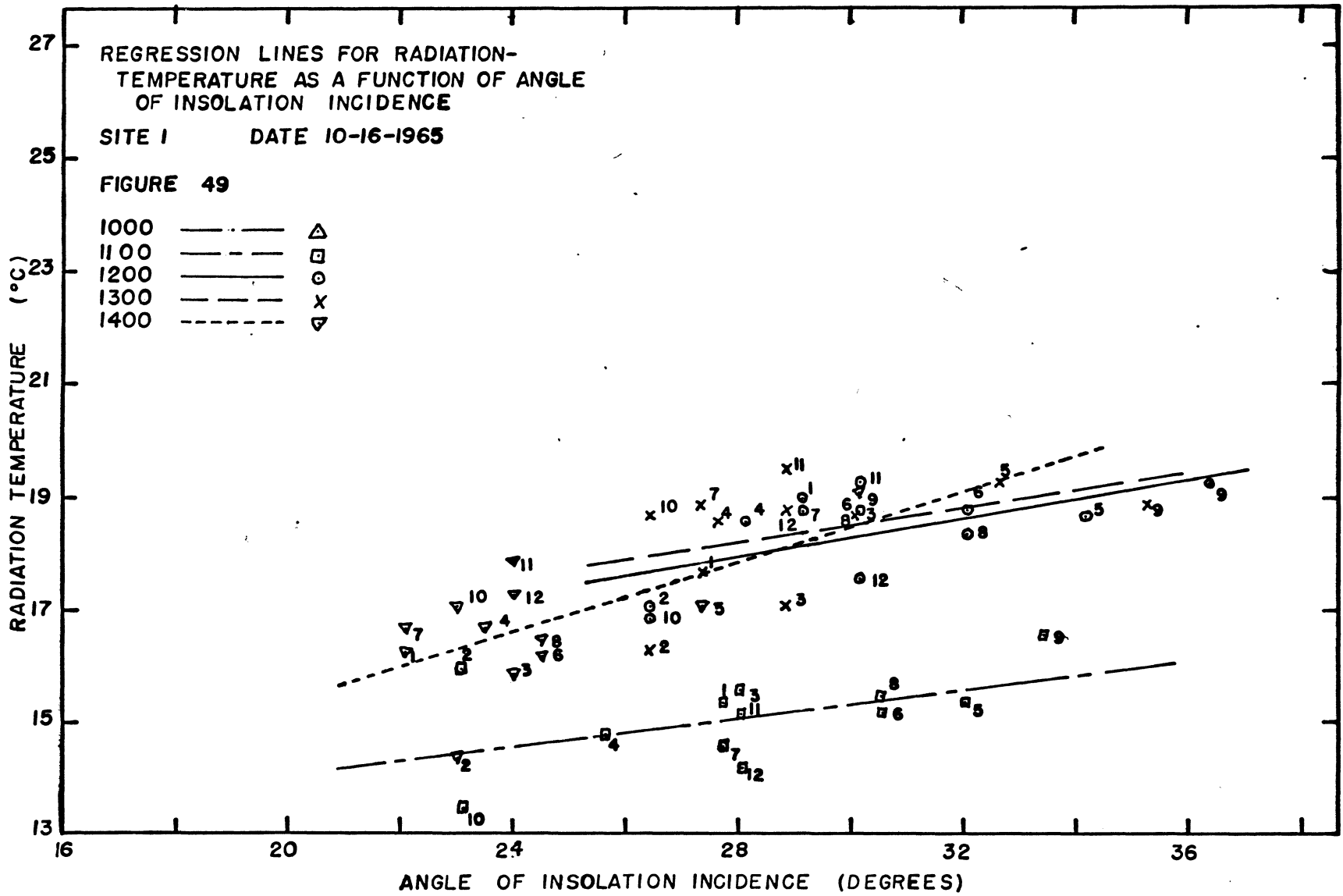


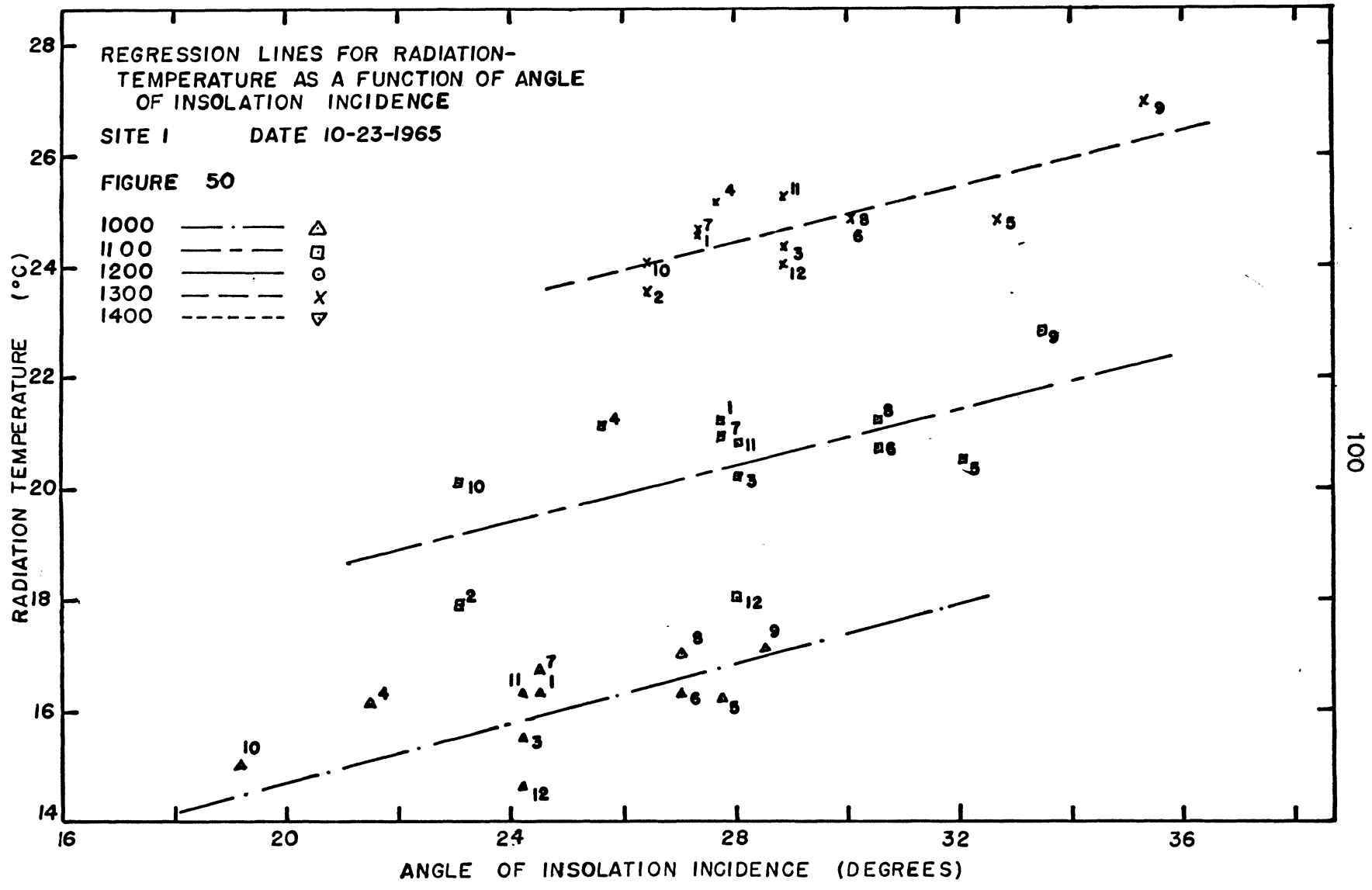


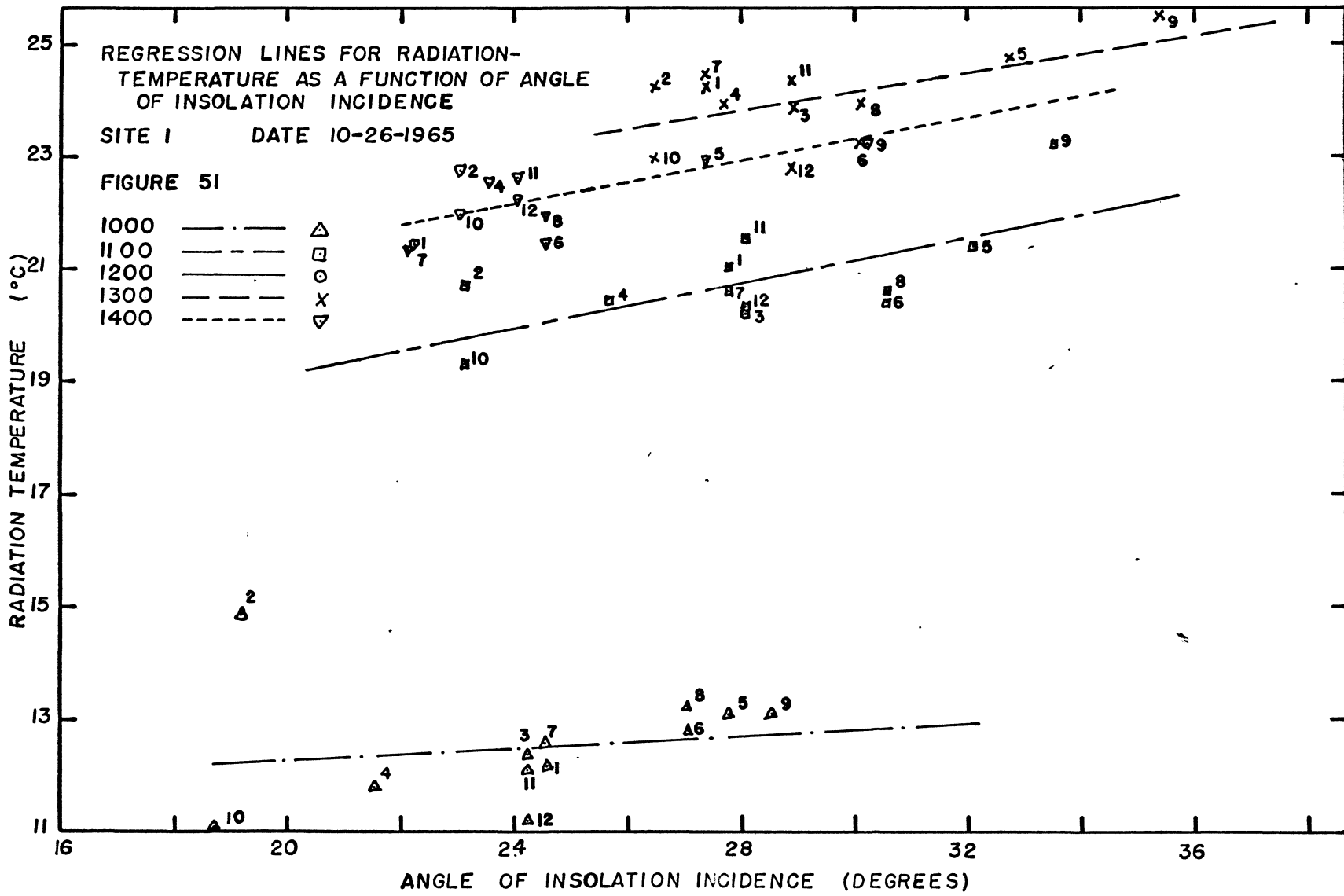
H. REGRESSION LINES FOR SITE I FOR FIVE DAYS













I. SCATTER DIAGRAMS OF RADIATION-  
TEMPERATURE DEVIATES

